

# Computational Studies on Five Membered Heterocyclic Open-Shell Systems and Setting up of Matrix Isolation IR Spectroscopy

AJIT KUMAR YADAV

MS12024

*A dissertation submitted for the partial fulfilment  
of  
BS-MS dual degree in science*



INDIAN INSTITUTE OF SCIENCE EDUCATION AND RESEARCH, MOHALI

APRIL 2017

*To,*  
*My Family*

# CERTIFICATE OF EXAMINATION

This is to certify that the dissertation titled “**Computational Studies on Five Membered Heterocyclic Open-Shell Systems and Setting up of Matrix Isolation IR Spectroscopy**” submitted by Mr. Ajit Kumar Yadav (Registration Number: MS12024) for the partial fulfilment of BS-MS dual degree programme of Indian Institute of Science Education and Research, Mohali has been examined by the thesis committee duly appointed by the institute. The committee finds the work done by the candidate satisfactory and recommends that the report be accepted.

Dr. Sugumar Venkataramani

(Supervisor)

Prof. K. S. Viswanathan

(Committee member)

Dr. P. Balanarayan

(Committee member)

Dated:

# DECLARATION

The work presented in this dissertation has been carried out by me under the guidance of Dr. Sugumar Venkataramani at the Indian Institute of Science Education and Research, Mohali. This work has not been submitted in part or in full for a degree, a diploma, or a fellowship to any university or institute. Whenever contributions of others are involved, every effort is made to indicate this clearly, with due acknowledgement of collaborative research and discussion. This thesis is a bonafide record of original work done by me and all sources listed within have been detailed in the bibliography.

Ajit Kumar Yadav  
(Candidate)

Dated:

In my capacity as the supervisor of the candidate's project work, I certify that the above statements by the candidate are true to the best of my knowledge.

Dr. Sugumar Venkataramani  
(Supervisor)

# ACKNOWLEDGEMENTS

First and foremost, I want to express my profound gratitude toward my thesis supervisor and mentor Dr. Sugumar Venkataramani for always believing in me, encourage and motivate me throughout my project. I also want to thank Prof. K. S. Viswanathan and Dr. P. Balanarayan for being a part of my thesis committee and always available for valuable suggestions and discussions.

I pay respect and thankful to my lab members Sudha Patel, Chitranjan Sah (Changu), Mayank Saraswat (Mangu), Lilit Jacob (Baba), Ankit Gaur, Pravesh Kumar, Surbhi Grewal, Debapriya Gupta, Anjali Srivastava, Anjali Mahadevan (Bro), Athira T. John and Himanshu Kumar (B.Tech) for providing friendly environment in the lab. I want to use this opportunity to specially thank Changu, Mangu and Baba for helping me in my project. I also want to thank Changu for taking care of my fitness, Mangu for paying for my coffee and baba for all love and support.

I would like to express my heartfelt gratitude toward my parents and my younger brother for always supporting me. Most importantly I want to thank all my friends specially RAINBOW.

Finally, I want to thank IISER Mohali for all the facility and DST, Government of India for the Inspire Fellowship that has helped in covering the large part of my academic expenses for my studies.

# LIST OF ABBREVIATIONS

<b>RSE:</b>	Radical Stabilization Energy
<b>ESP:</b>	Electrostatic Potential
<b>CASSCF:</b>	Complete Active Space Self Consistent Field
<b>NBO:</b>	Natural Bond Orbital
<b>(U)B3LYP:</b>	(Unrestricted) Becke, 3-parameter, Lee-Yang-Parr
<b>(U)M06:</b>	(Unrestricted) Minnesota functional 06
<b>(U)MP2:</b>	(Unrestricted) Møller–Plesset 2 perturbation theory
<b>cc-pVTZ:</b>	Correlation Consistent Polarized Valence only basis set Triple-Zeta
<b>(U)CCSD(T):</b>	(Unrestricted) Coupled Cluster Single and Double Substitutions with Triples
<b>SOMO:</b>	Singly Occupied Molecular Orbital
<b>LUMO:</b>	Lowest Unoccupied Molecular Orbital
<b>ESR:</b>	Electron Spin Resonance
<b>CIDNP:</b>	Chemically Induced Dynamic Nuclear Polarization
<b>CI:</b>	Configuration Interaction
<b>DFT:</b>	Density Functional Theory
<b>(U)HF:</b>	(Unrestricted) Hartree-Fock
<b>CC:</b>	Coupled Cluster
<b>CISD:</b>	Configuration Interaction Single and Double Substitutions
<b>PES:</b>	Potential Energy Surface
<b>MCSCF:</b>	Multi-configurational Self Consistent Field
<b>CSF's:</b>	Configuration State Functions

**TS:** Transition Space  
**TB:** Through Bond  
**BSE:** Biradical Stabilization Energy  
**BDE:** Bond Dissociation Energy

# LIST OF FIGURES

- Figure 1.1** Interplay of various factors influencing ground state spin multiplicities of biradicals and triradicals
- Figure 1.2** Classification of biradicals
- Figure 3.1** Optimized structure of pyrrole, furan, thiophene and borole and their radical isomers
- Figure 3.2** Spin densities of dehydro- pyrrole (**1a-c**), furan (**2b, 2c**), thiophene (**3b, 3c**), borole (**4a-c**) radicals at different levels of theory
- Figure 3.3** Electrostatic potential contours estimated at (U)B3LYP/cc-pVTZ level of theory
- Figure 3.4** CASSCF/cc-pVTZ//(U)B3LYP/cc-pVTZ orbitals of the dehydro- pyrrole, furan, thiophene and borole radicals
- Figure 3.5** Possible 1,2 H-shift pathways of pyrrole radical at (U)B3LYP/cc-pVTZ levels of theory
- Figure 3.6** Unimolecular decompositions pathways of **1b** and **1c** at UB3LYP/cc-pVTZ level of theory
- Figure 3.7** Important geometrical parameters of didehydropyrrole biradicals optimized at (U)B3LYP/cc-pVTZ level of theory
- Figure 3.8** Biradical stabilization energy (BSE) at (U)B3LYP/cc-pVTZ level of theory
- Figure 3.9** Singlet and triplet energy gap (in kcal/mol) of didehydropyrroles at (U)B3LYP/cc-pVTZ level of theory
- Figure 3.10** Bond dissociation energies of pyrrole and dehydropyrrole radicals at (U)B3LYP/cc-pVTZ level of theory
- Figure 3.11** Spin densities of didehydro-pyrrole at (U)B3LYP/cc-pVTZ level of theory
- Figure 3.12** Parts of matrix isolation setup



# LIST OF TABLES

- Table 3.1** Relative energy (kcal/mol) of radical isomers at different levels of theory
- Table 3.2** Radical stabilization energy (RSE) at (U)B3LYP/cc-pVTZ level of theory
- Table 3.3** Second order perturbation energy values of dehydro- pyrrole, furan, thiophene and borole radicals at (U)B3LYP/cc-pVTZ
- Table 3.4** NBO of didehydro pyrrole biradicals at (U)B3LYP/cc-pVTZ level of theory

# LIST OF SCHEMES

- Scheme 1.** Target systems (a) Mono-radicals. (b) Biradicals.
- Scheme 2.** (a) Parent heterocycles and their corresponding dehydro- pyrrole, furan, thiophene and borole radicals. (b) Didehydropyrrole biradical isomers

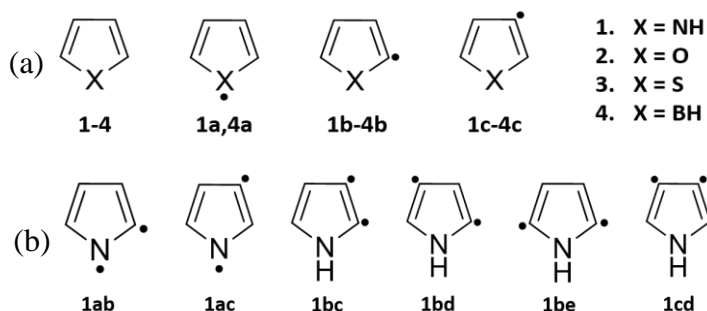
# CONTENTS

ACKNOWLEDGEMENTS	V
LIST OF ABBREVIATIONS	VI
LIST OF FIGURES	VIII
LIST OF TABLES	IX
LIST OF SCHEMES	X
<b>ABSTRACT</b>	<b>XIII</b>
<b>Chapter 1. Introduction</b>	<b>1</b>
1.1 General Introduction to Free Radical Chemistry	1
1.2 Heterocyclic Radicals	1
1.3 Approaches for High Spin Biradicals	2
1.4 Literature Background	3
1.5 Classification of Biradicals	4
1.6 Motivation	4
1.7 Approaches	6
<b>Chapter 2. Theoretical Insights and Computational Methods</b>	<b>7</b>
2.1 History and Developments in Computational Chemistry	7
2.2 Density Functional Theory	8
2.3 Methods	10
2.4 Basis Sets	10
2.5 Geometry Optimizations and Frequency Calculations	10
2.6 Natural Bond Orbital (NBO) Analysis	11
2.7 Multireference Calculations	11
2.8 Computational Details	13
<b>Chapter 3. Results and Discussion</b>	<b>14</b>
3.1 Five Membered Dehydroheterocyclic Radicals	14
3.1.1 Geometry	14

3.1.2 Stability Order	16
3.1.3 Radical Stabilization Energy Using Isodesmic Reaction	17
3.1.4 Spin Density	18
3.1.5 Electrostatic Potential	19
3.1.6 Multireference Calculations	21
3.1.7 Natural Bond Orbital (NBO) Analysis	23
3.1.8 Reactivity Studies of dehydropyrrole radicals	25
A. 1, 2 H- Shift	25
B. Unimolecular Decomposition Pathways	26
3.2 Didehydropyrrole Biradicals	28
3.2.1 Geometry	28
3.2.2 Biradical Stabilization Energy Using Isodesmic Reaction	29
3.2.3 Singlet-Triplet Energy Gap	30
3.2.4 Bond Dissociation Energy	30
3.2.5 Spin Density	31
3.2.6 Natural Bond Orbital (NBO) Analysis	32
<b>Chapter 4. Matrix Isolation Technique and Experimental Setup</b>	<b>35</b>
4.1 Matrix Isolation	35
4.2 Advantage of Matrix Isolation Technique	35
4.3 Instrumental Setup	35
4.3.1 Cryostat	36
4.3.2 Vacuum System	36
4.3.3 FTIR Spectrometer	37
<b>Chapter 5. Summary and Outlook</b>	<b>38</b>
5.1 Summary	38
5.2 Outlook	39
<b>References</b>	<b>40</b>
<b>Appendix</b>	<b>45</b>

# ABSTRACT

Computational studies of five membered mono-heteroatom containing heterocyclic radicals have been performed. Isomeric dehydro- pyrrole, furan, thiophene and borole radicals have been investigated. (**Scheme 1a**) These systems have been chosen to understand the effect of heteroatom in structural, stability and reactivity aspects of radicals. In this regard, we explored the ground state electronic structures and their geometrical parameters to get insights in to the structural aspects. Isodesmic reactions have been performed in order to get the radical stabilization energy (RSE) and overall stability order of the related radical species. Spin density and electrostatic potentials (ESP) have been computed in order to understand the localization of spin at the radical center and to get an overview of the electrostatic charges, respectively. Multiconfigurational CASSCF calculations and natural bond orbital (NBO) analysis have been performed for obtaining semi-quantitative information on the interaction between lone pair(s) of the heteroatom and radical electron. This information will be very useful in the fundamental point of view to understand whether such interactions provide stabilizing or destabilizing effects and also the mode of operation. In this regard, different levels of theory including (U)B3LYP/cc-pVTZ, (U)M06/cc-pVTZ, (U)MP2/cc-pVTZ and single point energy calculations at (U)CCSD(T)/cc-pVTZ and multireference CASSCF/cc-pVTZ methods have been used.



**Scheme 1.** Target systems (a) Mono-radicals. (b) Biradicals

Reactivity of dehydropyrrole radicals have also been investigated. In this regard, 1, 2 H-shift and unimolecular decomposition pathways have been calculated at (U)B3LYP/cc-pVTZ level of theory. Based on above electronic structural and reactivity informations, we

found out that nitrogen centred radical is the most stable among all possible isomeric radicals that we investigated. The reason is delocalization of radical electron in the ring that result in a p-character of SOMO. After this significant result, where we obtained a  $\pi$ -radical when the radical centre is created at nitrogen atom, we shifted our attention to create the spin interaction upon creation of another radical centre at carbon centres. In this regard, we extended this study to understand the ground state spin multiplicities of all possible didehydropyrrole biradicals. **(Scheme 1b)** Both singlet and triplet states for each pyrrole biradicals have been investigated in order to predict the ground electronic states. In this regard, we estimated the geometrical parameters, spin density, biradical stabilization energy, singlet-triplet energy gap, bond dissociation energy and natural bond orbital (NBO) at (U)B3LYP/cc-pVTZ level of theory. All these results show that all the biradicals with one of the radical centres at nitrogen atom are found to have triplet ground states. This provides an excellent chance for exploring new types of high spin systems.

Author has participated in the matrix isolation IR spectroscopy Installation.

# Chapter 1. Introduction

## 1.1 General Introduction to Free Radical Chemistry

Free radicals are one of the very important classes of reactive intermediates that contain unpaired electron(s) and are highly transient.<sup>1-3</sup> Generally synthetic chemists explore the radicals because they exist as the intermediate in many organic synthetic mechanisms.<sup>4-5</sup> For instance, several radical based reactions such as photo redox catalysis, radical addition and radical cyclization are of great importance in the field of organic synthesis.<sup>6</sup> The generation and reactivity of radicals play a crucial role in the combustion of petrochemicals. But the way of looking to the radicals changed when it receives the attention of biologist, polymer chemist and atmospheric chemist. They play an inevitable role in the synthesis of polymers<sup>7-8</sup> and atmospheric chemistry.<sup>9-10</sup> Equally they also play a vital role in biochemistry of diseases and ageing.<sup>11-12</sup> Generally free radicals are highly reactive and unstable but some of the stable radicals are also synthesized. So far the popular strategies for obtaining stable radicals are either to create radical centres at heteroatoms or through incorporation of conjugation to provide resonance conditions.<sup>13-14</sup> Due to these reasons heterocyclic radical are point of attraction for many theoreticians and experimentalists.<sup>15-17</sup> To understand the structural and reactivity aspects of radicals many synthetic methods like radical traps,<sup>18</sup> and radical clocks<sup>19</sup> and experimental techniques such as electron spin resonance (ESR),<sup>20</sup> chemically induced dynamic nuclear polarization (CIDNP), matrix isolation, mass spectrometry, photoelectron spectroscopy and other spectroscopic techniques along with computational methods play a significant role. Using these methods many studies have been done which range between monoradical to polyradicals.<sup>21-26</sup>

## 1.2 Heterocyclic Radicals

However, only limited progress have been made in the understanding of their heterocyclic analogues. Not only the parent heterocyclic radicals but their ring opening products and fragments are also important in astrochemical point of view.<sup>27</sup>

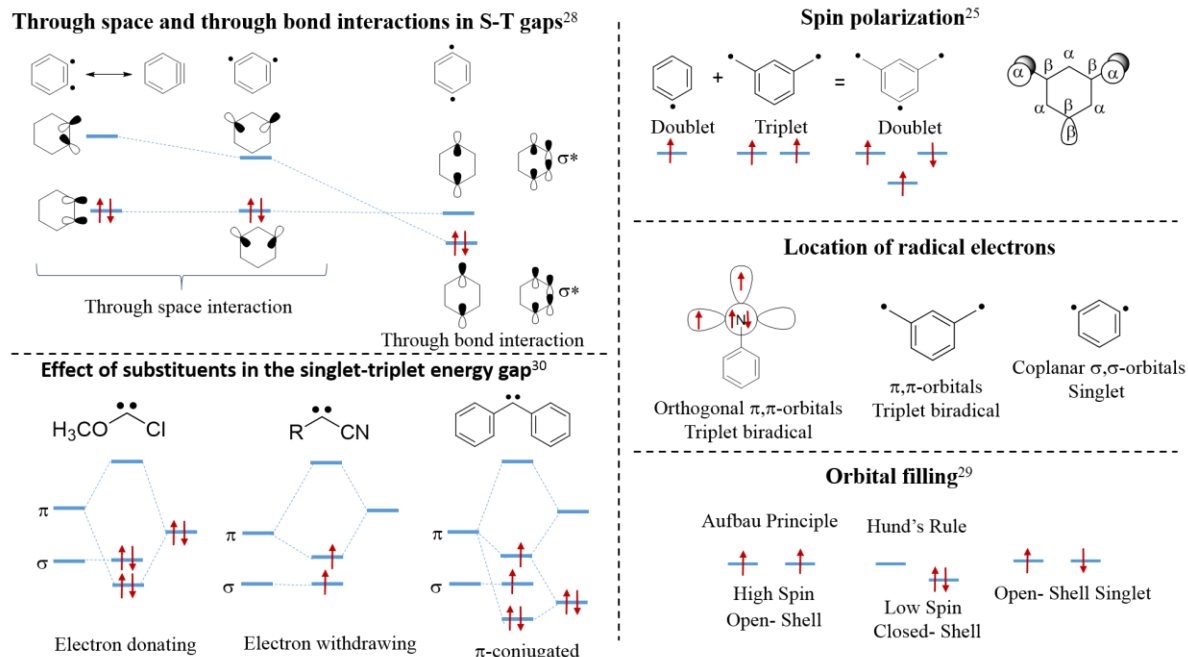
Among many heterocyclic radicals five membered heterocyclic radicals like pyrrole, thiophene, furan and borole containing nitrogen, sulphur, oxygen and boron as heteroatoms,

respectively. They are very important to understand the radical stability, reactivity and radical electron's interaction with the lone pair(s) of heteroatoms (if available). All these five membered heterocyclic radicals i.e. pyrrole, furan, thiophene and borole has three (**1a-c**), two (**2b-c**), two (**3b-c**) and three (**4a-c**) possible radical isomers, respectively. The presence of a hetero atom, in particular lone pair can influence a radical either spatially (through space interactions) or through intervening bonds (through bond interactions).<sup>28</sup> Such interactions are gaining valuable insights considering the stability of heterocyclic radicals are crucial to many biochemical processes and metabolism.

### 1.3 Approaches for High Spin Biradicals

These heterocyclic systems become even more interesting when biradicals are generated on them. Biradicals are generated by creating additional radical centers to any of the previously mentioned radicals. Due to the presence of lone pair, a potential three centered – four electron interactions can be possible, which results in multiconfigurational biradicals. Apart from through space and through bond interactions between the radical-radical interactions the lone pairs can also compete with them. Also, the domination of either Hund's rule or Aufbau principle will dictate the ground state electronic structure of the biradicals.<sup>29</sup> In principle, there are several biradicals that are known to exist with ground state singlet and triplets. Apart from the above mentioned reasons, spin polarization, residing orbitals in which the unpaired electrons are located, orbital interactions and also influence of the neighbouring functional groups can alter the ground state spin multiplicities. Few illustrations for such behaviour are shown in the **figure 1.1**. Due to the presence of such competing mechanisms, the investigations on biradicals provide curiosities for both theory as well as experiments.





**Figure 1.1** Interplay of various factors influencing ground state spin multiplicities of biradicals and triradicals.

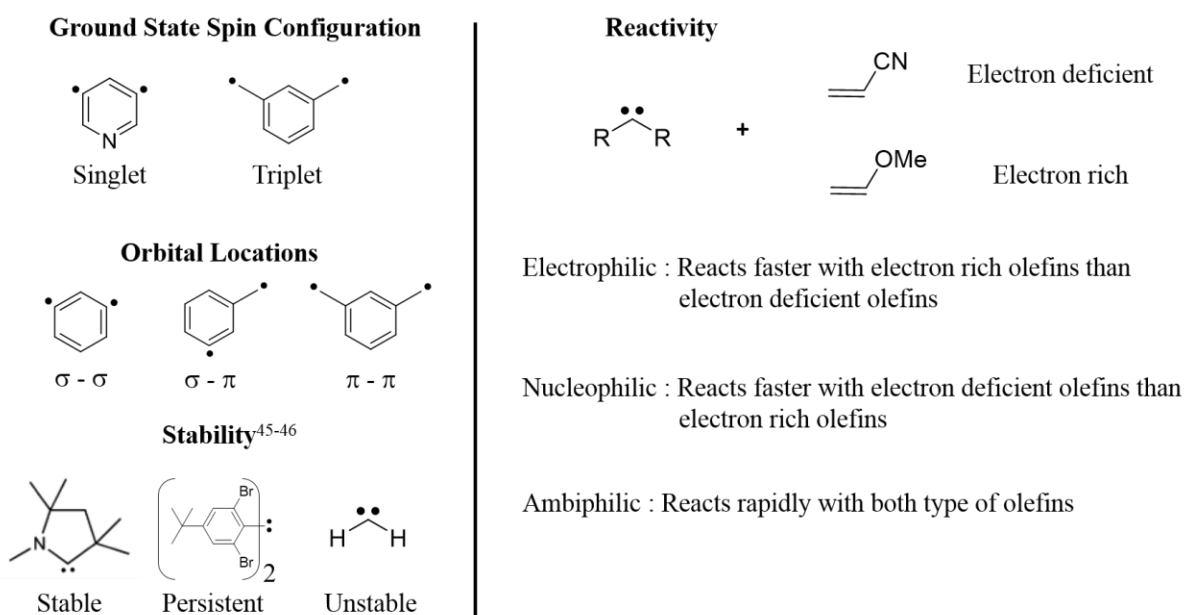
## 1.4 Literature Background

Many experimental and computational studies related to pyrrole, furan, thiophene and borole and their radicals have been reported. Dubnikova and Lifshitz have performed calculations on isomerization of pyrrole. They did Density functional theory (DFT) calculations including configuration interaction (CI) to investigate the pathways of the unimolecular isomerizations of pyrrole.<sup>31</sup> In another work, they also studied the ring expansions in *N*-methylene pyrrole, 2-methylene pyrrole, and 3-methylene pyrrole radicals.<sup>32</sup> Theoretical studies on mechanistic pathways based on pyrolysis of pyrrole have been investigated by Lei Zhai et al. using DFT studies.<sup>33</sup> McMahon and coworkers on their attempts to generate 2,5-didehydrothiophene using matrix isolation infrared spectroscopy, instead they ended up with its ring opening products.<sup>34</sup> The kinetics study of pyrolysis of furan has been theoretically performed by ab initio quantum chemical techniques and by detailed chemical kinetic modeling.<sup>35</sup> Braunschweig and coworkers demonstrated that the ground states of cyclopentadienyl cation and borole as triplet and singlet states, respectively using ESR spectroscopy.<sup>36</sup> Dongmei Lu et al. have reported that boron centered radicals undergoes a

radical electron flip to the empty orbital of boron and consequently the electron delocalized in the ring resulting in  $\pi$  character. This was extensively studied by looking at the spin densities of various boryl radicals.<sup>37</sup> Bond dissociation energies of pyrrole, furan and thiophene are reported by Yong Feng et al.<sup>38</sup> Several biradicals like carbenes, nitrenes, benzyne (1,2-, 1,3- and 1,4-didehydrobenzenes) and their corresponding heterocyclic analogues, didehydropyridines are subjected to many experiments and theoretical studies.<sup>39-44</sup>

## 1.5 Classification of biradicals:

Several biradicals have been classified into different groups in **(Figure 1.2)** based on various factors like ground state spin configuration, orbital locations and stability and also reactivity.

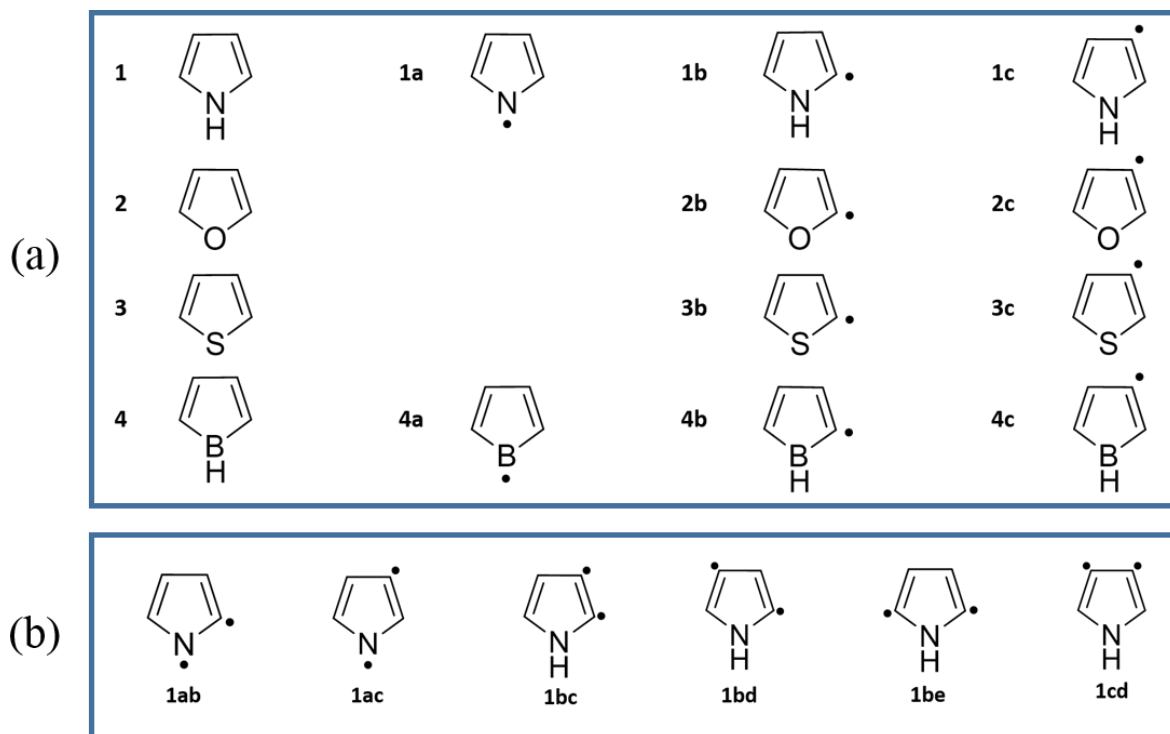


**Figure 1.2** Classification of biradicals

## 1.6 Motivation

Heterocyclic radicals have been subjected to many experiments such as pyrolysis, photolysis, unimolecular decomposition pathways, owing to their intermediacy in combustion chemistry of fossil fuels and atmospheric chemistry.<sup>9-10</sup> Apart from that theoretical studies on

selected heterocyclic radicals have been performed to understand the above mentioned results. Despite the presence of enormous studies, fundamental aspects such as interaction of lone pair of the heteroatoms with radicals with respect to the structural, stability and reactivity aspects are largely unknown. In our group, we are investigating various heterocyclic radicals containing with different numbers of heteroatoms. Besides, the formation of various possible ring opening products as a result of decomposition channels, and their spectral properties are very interesting in the astrochemical point of view. In this regard, we have chosen five membered dehydroheterocyclic radicals with one heteroatom as our targets. (**Scheme 2a**) During the investigations, we found out that the nitrogen centered radicals of pyrrole **1a** was found to have  $\pi$ -character with the formal radical center at the nitrogen is delocalized into the pyrrole ring. This motivated us to study the spin behavior of resulting biradicals when two radical centers are created in pyrrole ring, where one of the radical centers is at nitrogen. In this regard, we have chosen all the didehydropyrrole biradical isomers and subjected to computational studies. (**Scheme 2b**)



**Scheme 2.** (a) Parent heterocycles and their corresponding dehydro- pyrrole, furan, thiophene and borole radicals. (b) Didehydropyrrole biradical isomers

## 1.7 Approaches

To understand dehydro- pyrrole, furan, thiophene and borole radical isomers many computational approaches have been used. In this regard, we explored the ground state electronic structures and their geometrical parameters to get insights in to the structural aspects. Isodesmic reactions have been performed in order to get the radical stabilization energy (RSE) and overall stability order of the related radical species. Spin density and electrostatic potentials (ESP) have been computed in order to understand the localization of spin at the radical center and to get an overview of the electrostatic charges, respectively. Multiconfigurational CASSCF calculations and natural bond orbital (NBO) analysis have been performed for obtaining semi-quantitative information on the interaction between lone pair(s) of the heteroatom and radical electron. Similarly to understand didehydropyrrole biradical, we estimated the geometrical parameters, spin density, biradical stabilization energy, singlet-triplet energy gap, bond dissociation energy and natural bond orbital (NBO).

# Chapter 2. Theoretical Insights and Computational Methods

## 2.1 History and Developments in Computational Chemistry

Computational chemistry, alternatively sometimes called as theoretical chemistry or molecular modeling. Chemical properties of atomic and molecular systems can be extensively simulated using computers. Computational chemistry started developing under the lights of theoretical chemistry and chemical physics. Due to the development of the quantum theory in 1920's, calculations of many molecular and atomic properties were possible. A breakthrough in this field came with the development of the Hartree-Fock equations in the year 1930. The history of *ab initio* computations lies in the implementation of the Hartree-Fock equations into computer programs. Quantum mechanical calculation on the H<sub>2</sub> molecule first published by James and Coolidge in the year 1933.<sup>47</sup> In 1950, they introduced Gaussian-type basis functions for simulating orbitals and in the following year the foundations of computational chemistry were laid by the development of the matrix version of HF method by Roothaan and his co-workers. Roothaan's equations are the backbone to several algorithms used in different computational suites used for *ab initio* calculations. Quantum mechanics thus developed a path that lead to the formation of computational Chemistry.<sup>48</sup>

Independently, in the year 1927, Thomas and Fermi developed a theory using statistical mechanics that could relate the electron density on a system with the average energy of the system. The theory remained relatively stagnant for a few decades till the celebrated Hohenberg-Kohn Theorem came into play. The Hohenberg-Kohn-Sham version of the theorem proved to be another breakthrough for computational chemistry. This theory used functional instead of the quantum mechanical wave function picture and was widely celebrated as the Density Functional Theory. DFT calculations can be extended to several large systems because it a method that is known for computational efficiency. It is the most widely used for electronic structure calculations of atoms, molecules, solids, nanomaterials, synthetic materials, biological molecules and surfaces. It was in the year 1998, Walter Kohn was awarded the Nobel Prize in Chemistry for “his development of the density-functional theory.”

From these calculations molecular properties such as structures, energies, frequencies, dipole moments and electron distribution can be obtained. With the advent of better technologies, computational efficiency and algorithms, computational chemistry has developed into an independent branch of chemical sciences. Hybrid theories combining DFT and quantum mechanical methods are very popular and have been exploited for analyzing our system of interest. Popular methods for analyzing molecular systems include Hartree-Fock (HF), Density Functional Approaches (and modifications), Møller Plesset Perturbation Theory (MPn), Minnesota Functionals (Myz), Configuration Interaction Method (CI), Coupled Cluster (CC), Multi-Configuration Self Consistent Field etc.

## 2.2 Density Functional Theory

In recent years density function method is one of the dominant quantum chemical calculation used in energy surface simulations. DFT method allows much larger systems to be treated than by traditional ab initio methods, while retaining much of their accuracy. Traditional wavefunction methods such as variational or perturbative methods can be applied to find highly accurate results on smaller systems. This provides benchmarks for developing density functionals, which can then be applied to much larger systems. But DFT is not just another way of solving the Schrödinger equation. Nor is it simply a method of parametrizing empirical results. Density functional theory is a completely different, formally rigorous, way of approaching any interacting problem, by mapping it exactly to a much easier-to-solve non-interacting problem. Its methodology is applied in a large variety of fields to many different problems, with the ground-state electronic structure problem simply being the most common.

To reduce the degrees of freedom of the system we use Born-Oppenheimer approximation. In DFT functional is electron density, which is instead a function of space and time. Unlike Hatree Fock dealing directly with the many body wave functions, electron density is used as the fundamental property in DFT method. Using electron density instead of wavefunctions significantly reduces the complexity of calculations. The many body electronic wavefunction is a function of  $3N$  variables, whereas the electron density is a function of only  $x, y, z$  co-ordinates.

Electron density  $\rho(\mathbf{r})$  can be written as

$$\rho(\mathbf{r}) = N \int |\Psi|^2 d\mathbf{x}$$

Where  $N$  is no of electrons and  $dx$  is the volume element and  $\rho(r)$  is the probability of finding  $N$  electrons. Unlike wavefunction, electron density is observable and can be measured experimentally using X-ray diffraction. The basic principle of DFT methods lies in Hohenberg and Kohn theorem and it states as “energy of a quantum mechanical system can be calculated in principle if one know the ground state electron density. The theorem also states that the ground state system of electron is a result of the position of nuclei.

$$\hat{H} = -\frac{\hbar^2}{2m_e} \sum_i \nabla_i^2 + \sum_i V(r_i) + \sum_{i \neq j} V(r_{ij})$$

The kinetic energy of electrons and electron-electron interactions adjust themselves to form external potential, which is coming from the nuclei ( $V_{\text{ext}}$ ). Once the  $V_{\text{ext}}$  starts functioning on system, every other term including electron density adjust themselves to produce the lowest possible total energy of the system. Since external potential is the only variable required in the equation, if we are able to determine  $V_{\text{ext}}$  we can solve the Hamiltonian for the system. The corresponding  $V_{\text{ext}}$  is obtained from the strength and steepness of the nuclear energy- radius curve of the respective molecule. Once we identify the Hamiltonian the energy can be determined by applying this into the Schrodinger equation. Hohenberg and Kohn also concluded that for a given electron density there is only one possible  $V_{\text{ext}}$  and Hamiltonian operator, which when we plugged into the Schrodinger equation will provide the lowest energy value of the corresponding molecule.

As DFT is a function of electron density the total energy of the system should be expressed in terms of electron density. In case of en-en interaction consider  $\rho(r)$  as a set of electrons in a vicinity of radius  $r$  and assume that each electron is interacting with the total electron density in that space. This particular interaction can be expressed using coulomb energy and the integration over all the electron gives us the complete electron-electron interaction energy. The  $V_{\text{ext}}$  can also be expressed as the product of nuclear position and electron density over the space. Even the kinetic energy term have been expressed as a function of electron density by a formula derived by Thomas Fermi. Conclusively DFT proves that each individual energy term can be expressed in terms of electron density and confirms the Kohn-Homberg theorem saying energy can be obtained from electron density.

To study defects in semiconductors density functional theory (DFT) is a major theoretical tool to calculate defect formation energy using more hybrid functional method.<sup>49</sup>

## 2.3 Methods

B3LYP is an extremely popular DFT method for *ab initio* computations. As described before, all DFT methods employ a functional approach and electronic properties of the system are determined from the electron density. The BLYP is one such functional which also includes some HF exchange. This includes the electron spin densities and their gradients. The most commonly used functional in this category is the B3LYP. The B3LYP includes the Becke three parameter non-local exchanges functional with the non-local correlation of Lee, Yang and Parr. B3LYP is famous because this was the 1<sup>st</sup> method which involved a significant improvement over Hartree Fock method. Moreover B3LYP is faster than most of the post HF methods and yields comparable results also. B3LYP was also a starting point for the development of many HF exchange correlation functional.<sup>50</sup>

## 2.4 Basis Sets

Basis sets cc-pVNZ where N=D,T,Q,5,6,...n (D=double-zeta, T=triple-zeta, etc.). The 'cc-p', stands for 'correlation consistent polarized' and the 'V' indicates they are valence only basis sets. Correlation consistent wavefunctions are optimized using CISD wavefunctions, which are geared towards recovering correlation energy of valence electrons. These wavefunctions are particularly designed to smoothly converge towards basis set limit. Redundant functions are removed from cc-pVTZ functions and has been rotated in order to increase the computational efficiency. These functions can be augmented with core functions for the calculation of geometric properties and with diffuse functions for the calculations of electronic excitation.<sup>51</sup>

## 2.5 Geometry Optimizations and Frequency Calculations

Optimization of molecular geometry involves investigating different possibilities of arrangements of atoms in space to attain the minimum energy state. This can be achieved by creating a potential energy surface. PES is a mathematical relation between different molecular



structure and their single point energies. Iterative self-consistent algorithms help to optimize a guess geometry into an energetically stable configuration. These algorithms trap critical points on the potential energy surface of the system. The minimum on the surface is the stable geometry in which the molecule may exist. The second derivative of the energy term at the critical point evaluates vibrational frequencies for that particular geometry. For a minimum, all frequencies of vibration should be positive whereas for other critical points like saddle points, there can be imaginary frequencies for one or more modes of vibration. The energy of the optimized structure is the energy that the suite calculates for the configuration at the optimized geometry.

Transition states structure can be determined by searching the saddle point in the potential energy surface. The 1<sup>st</sup> order saddle point corresponds to minimum in all direction except one. Second order saddle point is minimum in all direction except two and so on. Transition states are characterized by single imaginary frequency.

The energy should be corrected for zero point correction, and is referred to as zero point corrected energy.

## 2.6 Natural Bond Orbital (NBO) Analysis

Natural bond orbital analysis is based on the Bohr's atomic model and Lewis's shared electron pair model of chemical bonding.<sup>52</sup>

NBO Analysis is performed for radicals in order to understand the role of radical and lone pair (if available) interactions in the stability of the radicals and biradicals. Second-order perturbation energies of the various donor–acceptor orbital interactions can be computed as per the NBO analysis scheme. These orbital interaction energies are a function of both the energy difference between the donor and acceptor orbitals and their overlap. These calculations provide information on the orbital delocalizations responsible for the stability of a structure.<sup>53</sup>

## 2.7 Multireference Calculations

The basic method in computational chemistry which was used for a long time to compute the energies is self-consistent field (SCF) method. The first step of any quantum chemical calculation is the Hartree-Fock (HF) self-consistent field (SCF) method which

requires a single Slater determinant to optimize the orbitals with variation principle. In HF approximation method each electron is surrounded by the average potential of the remaining electrons without having a prior knowledge of the positions of these electrons. Because of this the Coulomb interaction and the exchange interaction between the electrons is taken into account in an averaged manner. One of the major drawback of HF approximation is overestimation of electron repulsion due to the electrons which are having opposite spin and unable to avoid each other when they come closer to each other. To overcome the electron correlation problems post Hartree-Fock methods were proposed for this kind of correlations of the electrons. Many post Hartree-Fock methods are available for e.g. Møller-Plesset (MP) perturbation theory, density functional theory (DFT), configuration interaction (CI), and coupled cluster (CC) methods which implemented for computations to approximate the wavefunction. For a defined basis set, post HF methods (correlation calculations) are usually much more expensive than a simple HF calculation. One should pay attention while analysing the HF calculation results because HF approximation use the single Slater determinant as zeroth order approximation which is only appropriate near to the equilibrium geometries.

The multiconfigurational self-consistent-field (MCSCF) method is very useful for those chemical systems in which a single electron configuration (or single Slater determinant) is no longer sufficient for the description of the electronic structure. This generally happens in the case of chemical reactions in which bonds breaking and formation involve for e.g. radicals, diradicals, polyradicals and metals of the first transition row. Complete active space SCF (CASSCF) is a special variant of MCSCF which requires a defined active space of certain electron and molecular orbitals.

Restricted Hartree-Fock (a single Slater determinant) wavefunction does not dissociate appropriately for homolytically cleavage of a bond for a closed-shell systems. Unrestricted formalism in Hartree-Fock methods provides a qualitatively good potential energy curve, but the results are not much accurate because in unrestricted formalism the wavefunction is no longer an eigenfunction of the spin operator. In order to keep a spin eigenfunction, we need to include more than one (at least two) determinants in our wavefunction so that it can dissociate homolytically for a closed-shell molecule. In the MCSCF method, the wavefunction is a linear combination of all possible Slater determinants (or configuration state functions, CSF's), and

then calculates the respective coefficients of all Slater determinant by variational method. However, the orbitals in CASSCF are obtained not as those that minimize the energy of a single Slater determinant, as in Hartree-Fock theory, but as those which minimize the energy of the MCSCF wavefunction.

## 2.8 Computational Details

All the calculations have been performed using Gaussian 09 software package.<sup>53</sup> Optimization of all the structures have been carried out at different level of theories like B3LYP, M06 and MP2 with unrestricted wavefunction for all the doublet states. Single point energy calculation are done at (U)CCSD(T) level using (U)B3LYP/cc-pVTZ optimized geometry. cc-pVTZ basis set have been used for all the calculations. Frequency calculation were also performed to confirm the optimized geometry as -minima. From natural bonding orbital (NBO) calculations with optimized geometry at (U)B3LYP/cc-pVTZ level of theory second order perturbation energy value have been computed.

To understand the molecular orbital multireference calculation have been carried out using MOLPRO software package.<sup>55-56</sup> For all the geometry optimized at (U)B3LYP/cc-pVTZ level of theory, a separate optimization and frequency calculation have been performed at CASSCF/cc-pVTZ level of theory using MOLPRO, using this energies of orbitals and occupancies of orbitals are estimated. To construct the active space, five  $\pi$ - orbital of ring, radical centered orbital and the orbital corresponding to lone pair(s) of heteroatom have been chosen, wherever necessary. The molecular orbitals have been visualized using Molden package.

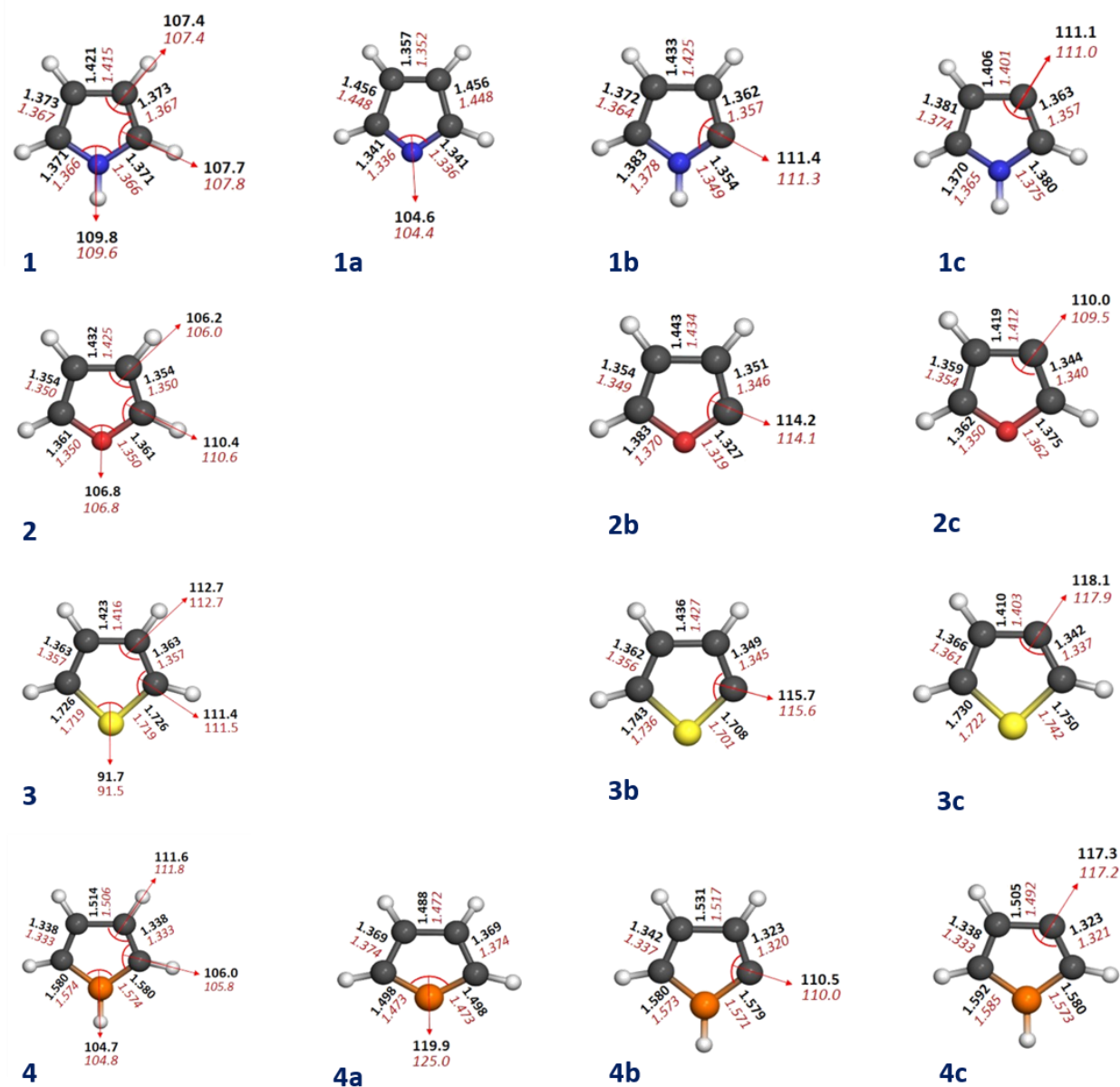
## Chapter 3 Results and Discussion

### 3.1 Five Membered Dehydroheterocyclic Radicals

Results of the electronic structure calculations at different levels of theory of all dehydro- pyrrole, furan, thiophene, and borole isomeric radicals along with their parent molecules are discussed in this section. Also, the reactivity aspects of pyrrole radicals have been shown and discussed at the end of this section.

#### 3.1.1 Geometry

Computational studies of all the isomeric dehydro- pyrrole, furan, thiophene, and borole radicals have been performed using different levels of theory. The optimized structures along with their significant geometrical parameters of all the radicals including their parent molecules are given in **figure 3.1**. All the molecules were optimized in either  $C_{2v}$  or  $C_s$  point group symmetries and possess a doublet spin. All the optimized geometries have been confirmed by frequency calculations (for the absence of imaginary frequency) for ensuring the minimum energy structures on the potential energy surface of respective molecule. We compared some key features of geometrical parameters of optimized structures of radical isomers with their respective parent molecule and observed that all these radicals follow some general trends. The bonds which are adjacent to the radical center got shortened in all the radicals irrespective of choice of heteroatom and alternate bond lengths relative to radical center are increased. Similarly, we also compared the bond angle at radical center and found that bond angle at radical center increases as compared to respective parent molecule except in case on N-centered radical i.e. **1a**, in case of **1a** bond angle at radical center decreases. Geometrical parameters have been estimated at both (U)B3LYP/cc-pVTZ and (U)M06/cc-pVTZ levels of theory . All these geometrical parameter trends are consistent with both levels of theory.

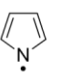
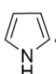
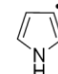

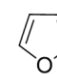
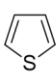
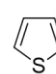
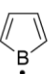
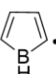
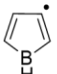


**Figure 3.1** Optimized structure of pyrrole, furan, thiophene and borole and their radical isomers. Selected geometrical parameters (bond distances in Å and bond angles in degrees) corresponding to the computational geometries at UB3LYP/cc-pVTZ (normal font) and UM06/cc-pVTZ (italics) level of theory are indicated.

### 3.1.2 Stability Order

We described the observed changes in geometrical parameters with respect to their parent molecule in previous section. In order to understand the relative stability pattern based on absolute energy within isomeric radical species for dehydro-pyrrole (**1a-c**), furan (**2b, 2c**), thiophene (**3b, 3c**), borole (**4a-c**) have been estimated at different levels of theory and their relative energies are listed in the **table 1**. Out of all the above-mentioned radicals, **1b, 1c, 2b, 2c, 3b, 3c, 4b, 4c** are carbon centered, which differs with their relative position from heteroatom. In case of pyrrole radicals **1a** has minimum energy and was found to be the most stable isomer followed by **1c** and **1b**, whereas **1b** and **1c** are very close in energy. The reason for **1a** to be most stable can be attributed to the delocalization of nitrogen centered radical in  $\pi$ -cloud of the ring. Energy difference between **1b** and **1c** lies between 0.0 to 0.5 kcal/mol depending upon levels of theory. In case of furan radicals, both isomers **2b** and **2c** are almost equal in energy and energy difference lies between 0.0 to 0.8 kcal/mol. Different levels of theory predicted different relative energies for **2b** and **2c**. In case of thiophene radicals **3c** is more stable compared to **3b** and energy difference is between 2.0 to 2.9 kcal/mol. In case of borole radicals **4a** is the most stable followed by **4c** and **4b**. Here also the reason for **4a** to be more stable is due to the delocalization of formal boron centered radical in the ring. All the levels of theory follow same trend in case of dehydro-pyrrole, thiophene and borole but in case of dehydro-furan there is some variations in (U)MP2/cc-pVTZ and single point energy calculation performed at CCSD(T)/cc-pVTZ/(U)B3LYP/cc-pVTZ levels as shown in the **table 3.1**

**Table 3.1** Relative energy (kcal/mol) of radical isomers at different levels of theory

Level of Theory	Pyrrole			Furan		Thiophene		Borole		
	 <b>1a</b>	 <b>1b</b>	 <b>1c</b>	 <b>3b</b>	 <b>3c</b>	 <b>4b</b>	 <b>4c</b>	 <b>5a</b>	 <b>5b</b>	 <b>5c</b>
UB3LYP/cc-pVTZ	0.0	24.7	24.3	0.1	0.0	2.9	0.0	0.0	11.1	7.4
UM06/cc-pVTZ	0.0	23.5	22.8	0.5	0.0	2.8	0.0	0.0	11.8	8.6
UMP2/cc-pVTZ	0.0	9.9	9.9	0.0	0.8	2.6	0.0	-	-	-
CCSD(T)/cc-pVTZ//UB3LYP/cc-pVTZ	0.0	25.0	24.5	0.0	0.04	2.0	0.0	0.0	8.7	6.1

### 3.1.3 Radical Stabilization Energy (RSE) Using Isodesmic

#### Reaction

We obtained of relative stability details of various radical isomers based on their absolute energy in previous section. In this section, we describe the relative stability based on radical stabilization energy. For that we used isodesmic reaction. The term “isodesmic” was first introduced by the quantum chemists Hehre, Ditchfield, Radom, and Pople in their publication in 1970.<sup>57</sup> An isodesmic reaction is a hypothetical reaction (not existing in reality) in which the same type of bond breaking and bond formation takes place on either side the reaction. This method is used to calculate the radical stabilization energy (RSE) for all the radical isomers. The enthalpy change ( $\Delta H_{298}$ ) during the hypothetical reaction is accounted for radical stabilization energy. In this regard, we considered benzene and radical isomers as reactants and the reaction yields the phenyl radical and parent heterocyclic molecule as products. In the whole process radical has been transferred from heterocyclic molecule to benzene. Estimated RSE values are listed in **table 3.2** at (U)B3LYP/cc-pVTZ level of theory.

**Table 3.2** Radical stabilization energy (RSE) at (U)B3LYP/cc-pVTZ level of theory

	 <b>1a</b>			 <b>1b</b>		 <b>1c</b>		 <b>3b</b>		 <b>3c</b>		 <b>4b</b>		 <b>4c</b>		 <b>5a</b>			 <b>5b</b>		 <b>5c</b>	
$\Delta H$ (kcal/mol)	17.2	-7.7	-7.1	-7.9	-7.8	-5.9	-3.0	9.4	-1.7	1.8												
Relative energy (kcal/mol)	0.0	24.7	24.3	0.1	0.0	2.9	0.0	0.0	11.1	7.4												

From the RSE values, it is clear that **1a** is the most stable radical as it has the highest positive  $\Delta H$  value, which implies that reaction is favorable in the backward direction that is

the formation of radical. This may be due to the delocalization of radical in the ring and **2b** is the least stable radical among all the radical isomers with a relatively large negative  $\Delta H$  value. **4a** is the second most stable radical and it may also have some delocalization in the ring but not as much as compared to **1a**. Based on these isodesmic reactions, we found out that relative stability based on radical stabilization energies of all the heterocyclic radicals follows the same trend as the comparison of absolute energy (U)B3LYP/cc-pVTZ level of theory.

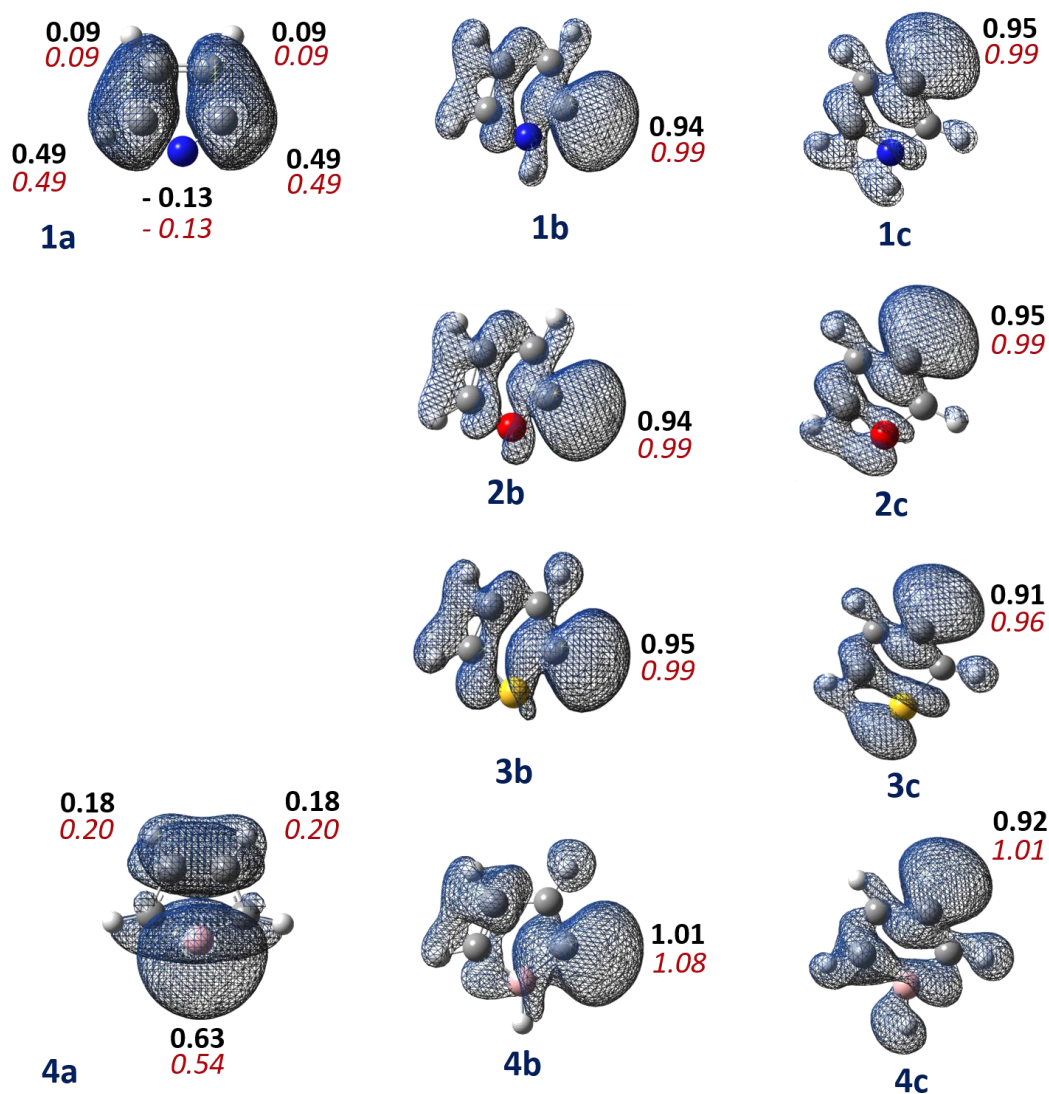
### 3.1.4 Spin Density

Spin density is the total electron spin of the free radical defined as the electron density of one spin (beta spin) subtracted from the electron density of opposite spin (alpha spin). Analysis of spin density illustrates how the electron spin at the radical center is distributed whether it is localized or delocalized and also provides qualitative information about the interaction of radical electron with other atoms in this particularly with heteroatom. The spin density of all the radical isomers have been estimated at UB3LYP/cc-pVTZ and UM06/cc-pVTZ levels of theory and the results are shown in **figure 3.2**. The observations depict that all the carbon centered radicals (**1b**, **1c**, **2b**, **2c**, **3b**, **3c**, **4b** and **4c**) carries a large positive spin density value at the formal radical centers, which suggests that these radical spins are localized. On the other hand, the N-centered radical **1a** and B-centered radical **4a** follows a different trend. In case of **1a** the formal radical center has a negative spin density value and all the other carbon centers poses a positive spin density. This spin density values implies that the spin density and the resulting radical character is delocalized over the ring. Similarly the carbon centers show a positive spin in **4a**, however, unlike N-center the B-center depicts a positive spin density, which is higher than the C-centers. This indicates that delocalization of radical character towards the carbon atom takes place in **4a** also but to a lesser extent as compared to **1a**.

The higher spin density at formal radical centers can be correlated with higher reactivity of the radical. The stability order follows the above trend with spin density in the radical isomers except in **1b**, **1c** and **2b**, **2c** radical isomers. However these radicals comprise spin densities with negligible difference, which is acceptable as the relative energy difference



among these radicals are trivial. The larger degree of stabilization in **1a** and **4a** can also be explained using the distribution of spin and radical character throughout the molecule.



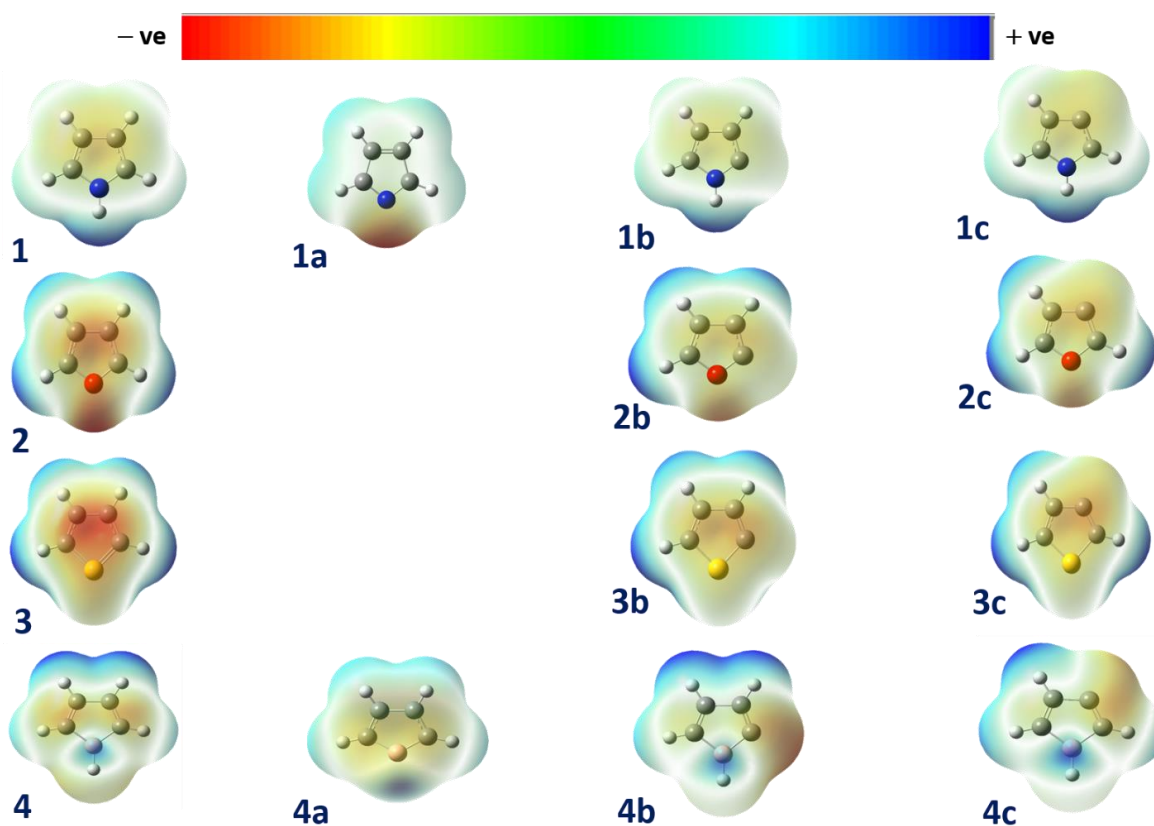
**Figure 3.2** Spin densities of dehydro-pyrrole (**1a-c**), furan (**2b, 2c**), thiophene (**3b, 3c**), borole (**4a-c**) radicals at different levels of theory (The most significant spin density values of each molecule are indicated; UB3LYP/cc-pVTZ (normal font) and UM06/cc-pVTZ (italics) levels of theory).

### 3.1.5 Electrostatic Potential

Electrostatic potential (ESP) can be defined as the force experience by a unit positive charge at any point in the space. ESP acts as a good guide in predicting the reactivity of the molecule towards positive and negatively charged reactants. If the ion is attracted to the molecule then the potential is negative. If the ion is repelled by the molecule then the potential is positive. Since the ion has a unit positive (+1) charge, it will be attracted to electron-rich regions of the molecule and repelled by electron-poor regions. Thus, electron-rich regions usually have negative potentials and electron-poor regions usually have positive potentials. The three dimensional diagram of the ESP distribution known as electrostatic potential map helps in understanding the charge distribution and other charge related properties of the molecule.

By using the ESP surface one can easily identify the electron rich and deficient regions according to the colour variation. The ESP map can also be used to understand the nature of chemical bond. Molecule with great electronegativity difference indicate that the bond is more polarized and greater extent of intermediate regions indicates less polarized bonds.

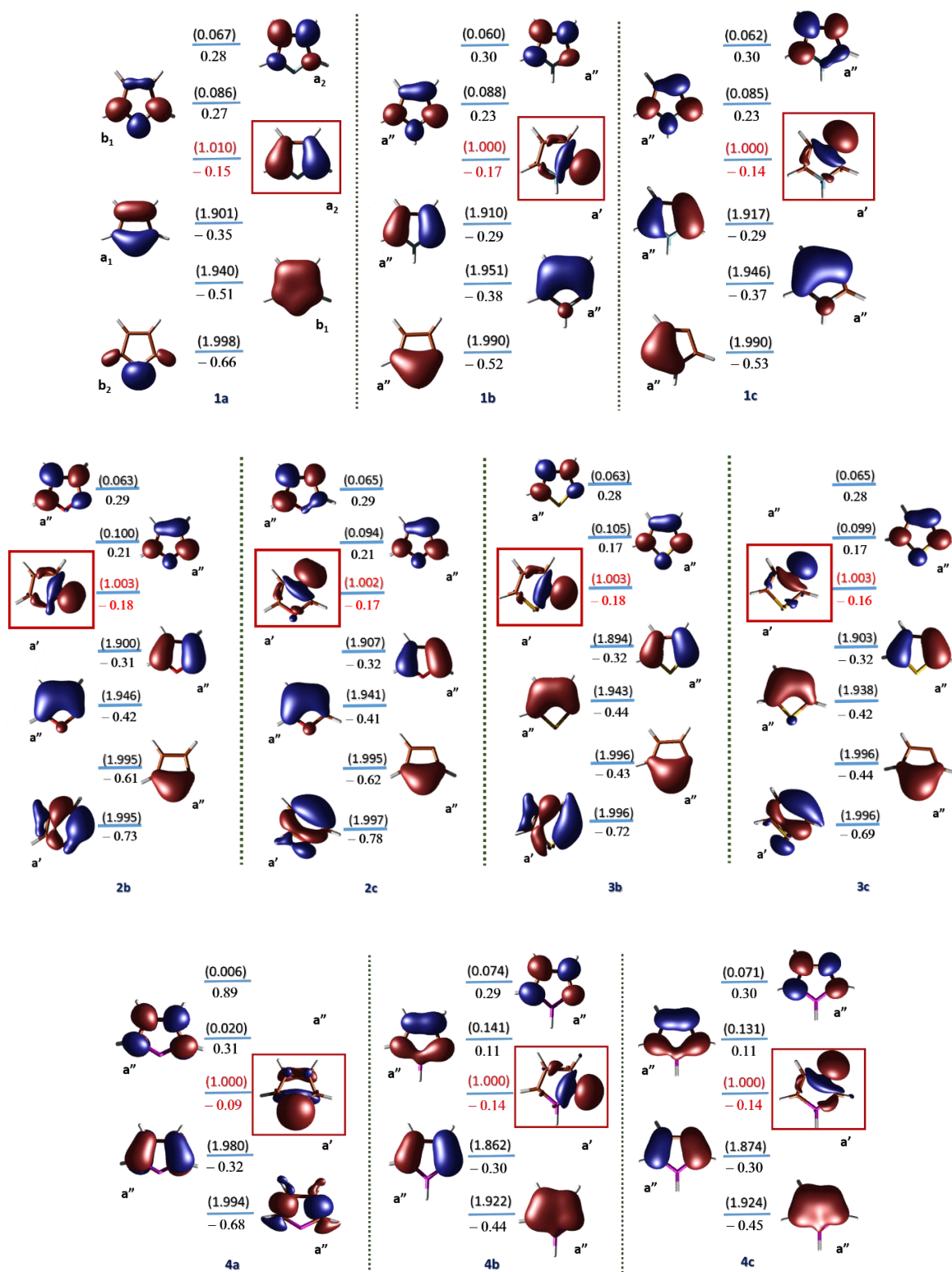
The three dimensional potential diagram of all the radical isomers and their respective parent molecules are generated and plotted in **figure 3.3**. The map indicates that oxygen and sulphur atoms in furan and thiophene radical isomers, respectively, pose a great negative potential because of the lone pair of electrons. Similarly radical center also depicts a negative potential for all the carbon centered radical as expected, which confirms the results from spin density calculations. In case of B-centered radical **4a** a negative potential is observed to be delocalized over the carbon centers. In contrary, the ESP map shows a localized electron density only at the N-atom in **1a**, even though the spin density values suggests delocalization of spin, an indication of the presence of lone pair of electrons in the sigma plane.



**Figure 3.3** Electrostatic potential contours estimated at (U)B3LYP/cc-pVTZ level of theory (the contour has been plotted with an isovalue 0.02 and density 0.0004)

### 3.1.6 Multireference Calculations

To understand the mode of operation and the influence of lone pair (if available) on stability, a qualitative study of the interaction between lone pair and the radical electron is required. In this regard, we performed optimization followed by frequency calculation at multireference electronic structure mode using CASSCF method. The spin densities which are shown earlier about the localization and delocalization of radical is supported by this calculation. For all the radicals, lone pair orbital (if available) are found to be low lying as compared to the  $\pi$ -orbitals.



**Figure 3.4** CASSCF/cc-pVTZ/(U)B3LYP/cc-pVTZ orbitals of the dehydro-pyrrole, furan, thiophene and borole radicals. SOMO have been highlighted by a box. All the orbitals have been rendered at an isovalue of 0.05

### 3.1.7 NBO Analysis

To find the interaction between the lone pair (if available) and the radical electron, and to quantify the interactions, we performed the NBO calculations at (U)B3LYP/cc-pVTZ level of theory. The NBO calculations have been carried out for all the radical isomers of pyrrole, furan, thiophene and borole and the results of interactions are shown below in **table 3.3**. Through this studies, we mainly focused on the interactions between the lone pair and the radical electron and the mode of interaction, i.e. through space (direct interaction) or through bond (indirect interactions through intervening bonds)

**Table 3.3** Second order perturbation energy values of dehydro- pyrrole, furan, thiophene and borole radicals at (U)B3LYP/cc-pVTZ

<b>1a</b>			<b>1b</b>			<b>1c</b>		
Interactions			Interactions			Interactions		
Donor NBO	Acceptor NBO	<E2>	Donor NBO	Acceptor NBO	<E2>	Donor NBO	Acceptor NBO	<E2>
n (N5)	$\pi^*_{C1-C2}$	3.82	n (N5)	$\pi^*_{C1-C2}$	15.85	n (N5)	$\pi^*_{C1-C2}$	20.03
n (N5)	$\pi^*_{C1-H6}$	1.28	n (N5)	$\pi^*_{C3-C4}$	19.79	n (N5)	$\pi^*_{C3-C4}$	13.25
n (N5)	$\pi^*_{C3-C4}$	3.82	$\pi^*_{C1-C2}$	$\pi^*_{C3-C4}$	27.3	$\pi^*_{C1-C2}$	$\pi^*_{C3-C4}$	32.35
n (N5)	$\pi^*_{C4-H9}$	1.28						

<b>2b</b>			<b>2c</b>		
Interactions			Interactions		
Donor NBO	Acceptor NBO	<E2>	Donor NBO	Acceptor NBO	<E2>
n1 (O8)	$n^*_{C4}$	2.51	n1 (O8)	$n^*_{C3}$	0.28
n1 (O8)	$\pi^*_{C3-C4}$	1.75	n1 (O8)	$\pi^*_{C3-C4}$	1.76
n2 (O8)	$\pi^*_{C3-C4}$	16.64	n2 (O8)	$\pi^*_{C3-C4}$	10.20
$\pi^*_{C1-C2}$	$\pi^*_{C3-C4}$	21.13	$\pi^*_{C1-C2}$	$\pi^*_{C3-C4}$	25.19

<b>3b</b>			<b>3c</b>		
Interactions			Interactions		
Donor NBO	Acceptor NBO	<E2>	Donor NBO	Acceptor NBO	<E2>
n1 S8	$\sigma^*_{C4}$	0.43	n1 S8	$\pi^*_{C3-C4}$	1.18
n1 S8	$\pi^*_{C3-C4}$	2.03	n2 S8	$\pi^*_{C3-C4}$	7.44
n2 S8	$\pi^*_{C3-C4}$	12.84	$\pi^*_{C1-C2}$	$\pi^*_{C3-C4}$	31.33
$\pi^*_{C1-C2}$	$\pi^*_{C3-C4}$	41.86			

<b>4a</b>			<b>4b</b>			<b>4c</b>		
Interactions			Interactions			Interactions		
Donor NBO	Acceptor NBO	<E2>	Donor NBO	Acceptor NBO	<E2>	Donor NBO	Acceptor NBO	<E2>
$n^*(1) B9$	$n^*(2) B9$	0.35	$n^* C4$	$\pi^* C3-C4$	0.32	$n^* C3$	$\pi^* C2-C3$	2.55
$n^*(2) B9$	$\pi^* C1-B9$	1.09	$n^* C4$	$\pi^* C4-B9$	1.15	$n^* C3$	$\pi^* C3-C4$	1.24
$n^*(2) B9$	$\pi^* C4-B9$	1.09	$n^* B9$	$\pi^* C3-C4$	3.25	$n^* B9$	$\pi^* C3-C4$	2.35

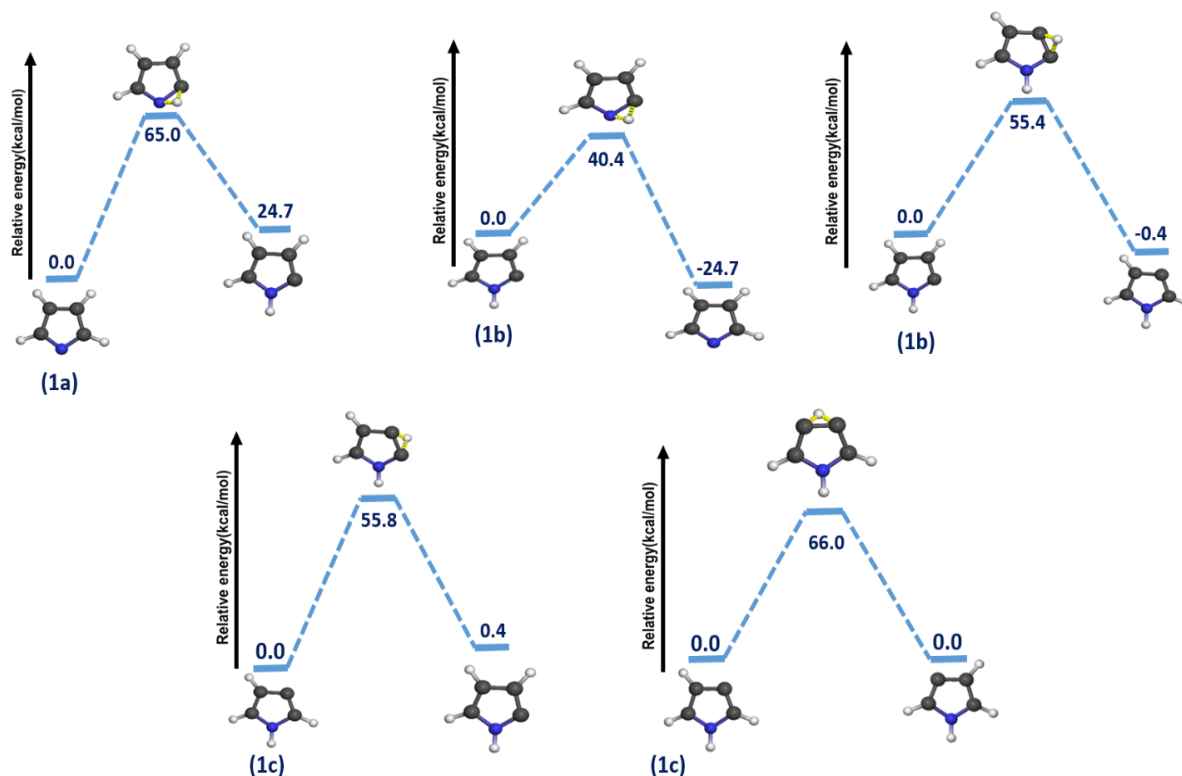
From the **Table 3.3**, we observed that the interaction energies corresponding to through space (TS) interaction are found to be either weak or completely absent. The reason for such ineffective spatial interaction can be attributed to the geometrical constraints. In the case of pyrrole radical, radical and lone pair orbitals are orthogonal to each other. In case of furan and thiophene radical electron and lone pairs are not in the same plane instead at an angle to each other. In case of borole there is no lone pair.

### 3.1.8 Reactivity Studies of dehydropyrrole radicals

The reactivity studies of dehydropyrrole radicals are essential in understanding the characteristics of ring opening products and comparing the kinetic stability of each radical. In this regard, four different approaches have been considered, which include isomerization through 1,2 H-shift, unimolecular decomposition to form ring opening products, C-H bond cleavage to form biradical and concerted ring opening channels. Isomerization through 1,2 H-shift and unimolecular decomposition studies of dehydropyrrole radicals been carried out and biradical studies of all the radicals will be discussed in part 2 of result and discussion. Despite multiple attempts, the reactivity channels through concerted mechanisms were not obtained.

#### A. 1, 2 H-shift

Inter conversion barrier between various isomeric radical through 1,2 H-shift have been carried out at (U)B3LP/cc-pVTZ level of theory and shown in **figure 3.5**. The radical isomer **1a** has only one possibility of H transfer, whereas **1b** and **1c** have two possibilities. The conversion of **1a** to **1b** is kinetically less favorable with a barrier of 65 kcal/mol. This is expected as the **1a** is the most stable radical isomer among pyrrole radicals. The H-shift from **1b** to form **1a** is the energetically most favorable pathway with the lowest energy barrier of 44 kcal/mol. The H-shift between **1b** and **1c** showed almost similar energy barrier (~55 kcal/mol) as both the isomers are energetically close. Surprisingly, the inter-conversion between the identical isomers (i.e. **1c** to **1c**) possess a transition energy barrier of 66 kcal/mol.



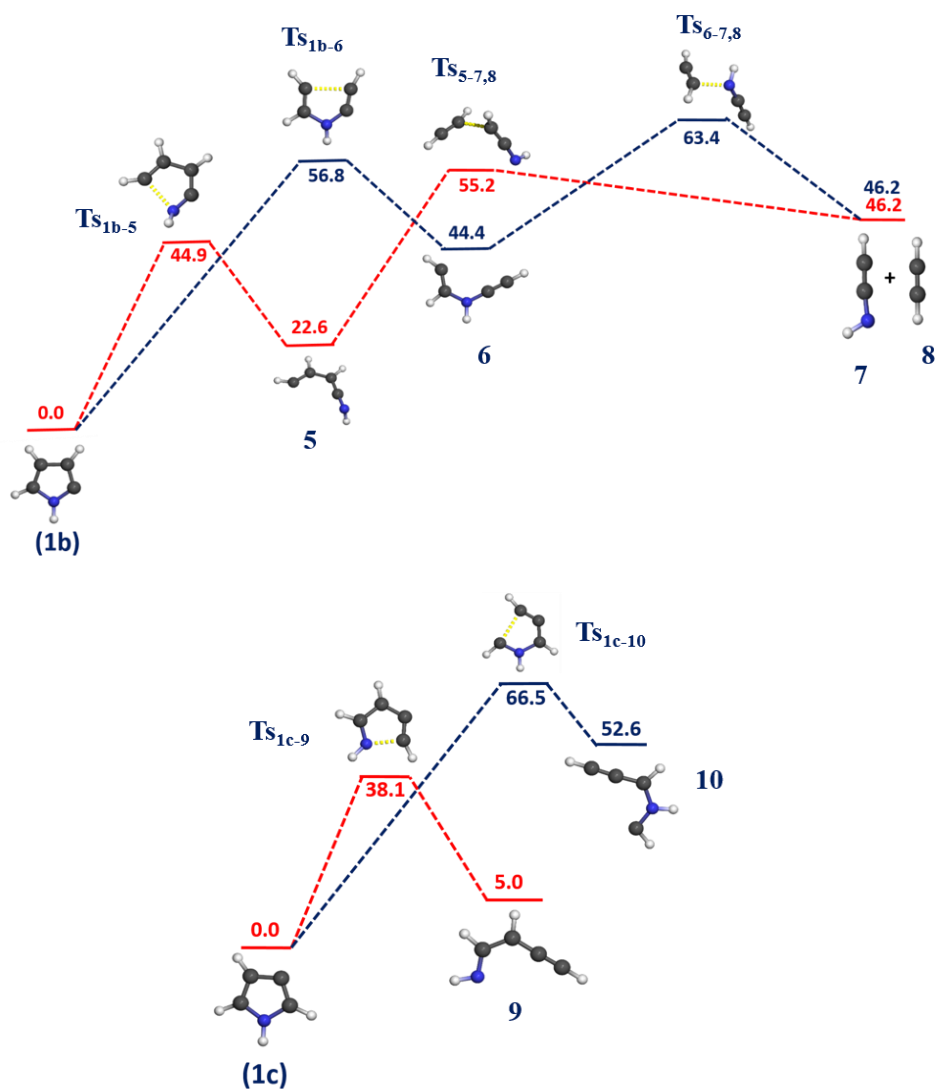
**Figure 3.5** Possible 1,2 H-shift pathways of pyrrole radical at (U)B3LYP/cc-pVTZ levels of theory.

## B. Unimolecular Decomposition Pathways

The investigation of unimolecular pathways are important in understanding the kinetic stability of the radicals and the products formed after the decomposition are of great importance in interstellar chemistry. In this aspect, we studied the unimolecular decomposition channels of all pyrrole radicals. However, we were unable to obtain any decomposition pathways for **1a** and the difficulty in obtaining the bond cleavage can be due to the extra stability of the radical isomer through the delocalization of electron density. The decompositions channels for both **1b** and **1c** have been estimated and are shown in **figure 3.6**. There are two ring opening possibilities for **1b** involving N1-C5 and C3-C4 bond cleavages. The N1-C5 bond cleavage is the energetically favorable pathway with an energy barrier of 44.9 kcal/mol. Whereas, the C-C bond breaking lies at a higher energy, which is 11.9 kcal/mol higher than the former. Both these pathways finally lead to the formation of acetylene and HNCCH radical. Similarly **1c** also has two decomposition pathways involving the breaking of N1-C2 and C4-C5 bonds. In



case **1c** also the cleavage of N-C bond is found to be thermodynamically more favorable than C-C bond cleavage with an energy barriers of 38.1 and 66.5 kcal/mol respectively. The intermediates formed from these transitions states are thermodynamically less stable as compared to the reactants. Although, the intermediate formed through the C-N bond cleavage has a comparable energy to the reactant, which is 5 kcal/mol higher than the later. In summary, the C-N bond cleavage in **1c** is the thermodynamically the most favorable pathway and C-C bond cleavage in **1c** is the least favorable channel.



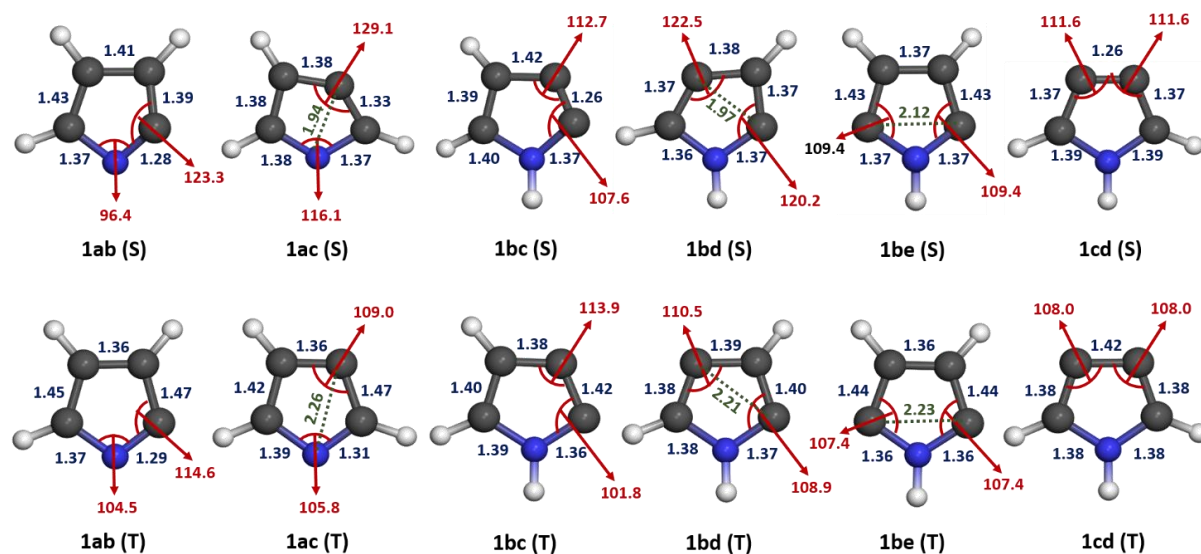
**Figure 3.6** Unimolecular decompositions pathways of **1b** and **1c** at UB3LYP/cc-pVTZ level of theory. All the energies values (in kcal/mol) mentioned are relative to the reactant.

## 3.2 Didehydropyrrole Biradicals

In this part of results and discussion, the electronic structural aspects, stability and also the ground state spin multiplicities of didehydropyrrole biradicals are discussed at (U)B3LYP/cc-pVTZ level of theory.

### 3.2.1 Geometry

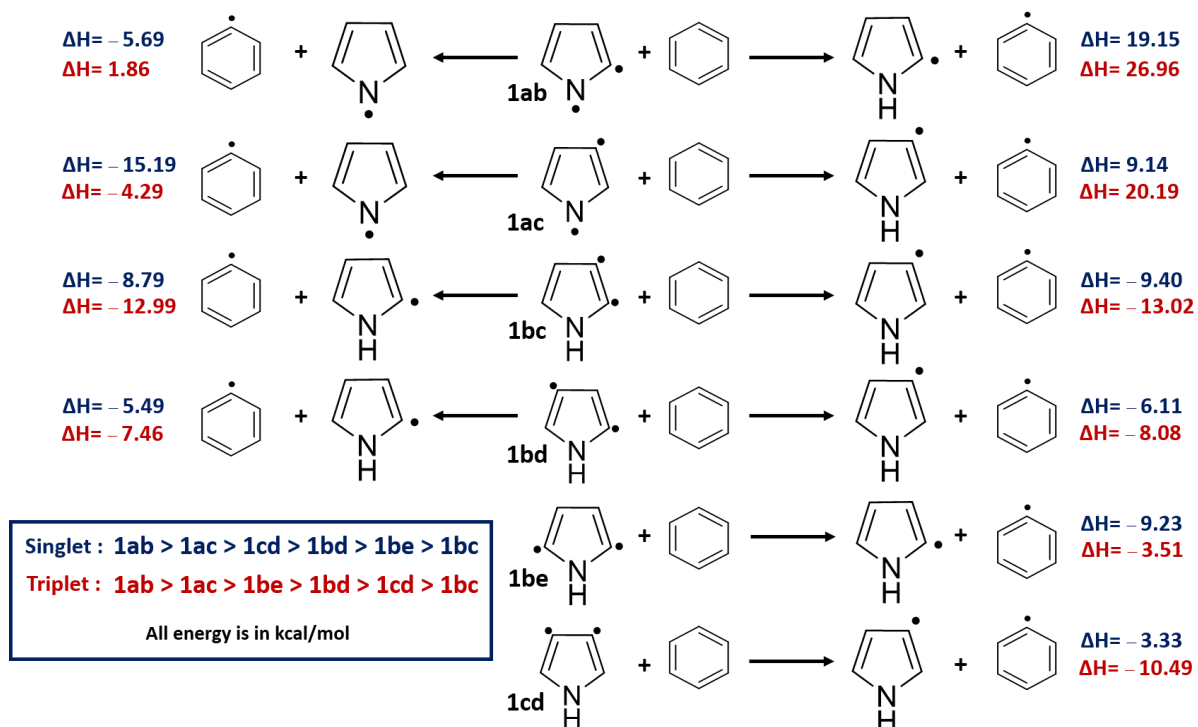
Computational studies of all the isomeric didehydropyrrole biradicals have been done using (U)B3LYP/cc-pVTZ level of theory. The optimized structures along with their geometrical parameters of all the biradicals with their parent molecules are given in **figure 3.7**. All the molecules have been optimized at their singlet as well as triplet states. All the geometrical optimizations have been confirmed by frequency calculations for ensuring the calculated structures as true minima in the potential energy surfaces of respective molecule. Upon comparing the geometrical parameters, we found out that whenever the two radicals in a molecule is at meta position to each other their internuclear distance decreases in singlet state and remain almost same in triplet state as compared to both the parent radicals.



**Figure 3.7** Important geometrical parameters of didehydropyrrole biradicals optimized at (U)B3LYP/cc-pVTZ level of theory, first row of the figure shows the singlet state and second row shows the triplet state of the corresponding didehydropyrrole biradicals.

### 3.2.2 Biradical Stabilization Energy Using Isodesmic Reactions

We once again used isodesmic reactions to calculate the relative stability order of all the biradicals at singlet and triplet states. The isodesmic reaction of all the singlet and triplet state of all the biradicals are shown in the **figure 3.8**.

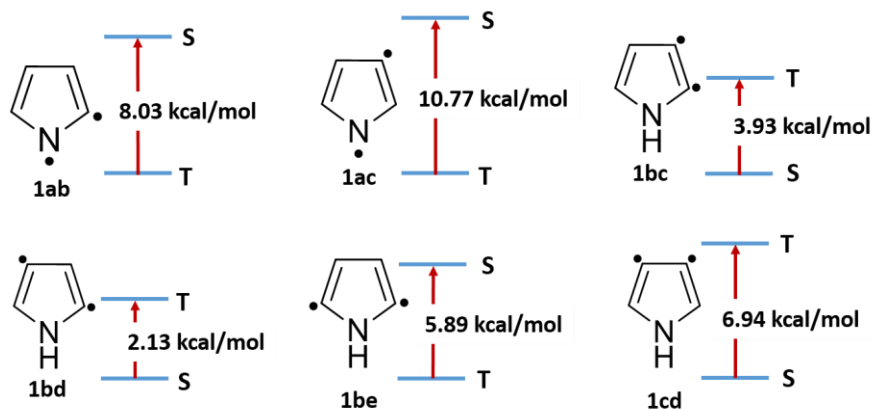


**Figure 3.8** Biradical stabilization energy (BSE) at (U)B3LYP/cc-pVTZ level of theory; Enthalpy changes (in kcal/mol) corresponding to singlet and triplet states of the biradicals are shown in blue and red colour, respectively.

From the **figure 3.8**, we obtained different stability order in singlet and triplet states of the biradicals. But we found out that the most stable biradicals are those biradicals where one radical is located at the nitrogen center of the molecule irrespective of the spin state.

### 3.2.3 Singlet-Triplet Energy Gap

To find which state of the biradical is stable, singlet and triplet energy gaps of all the didehydropyrroles have been calculated at (U)B3LYP/cc-pVTZ level of theory and shown in **figure 3.9**

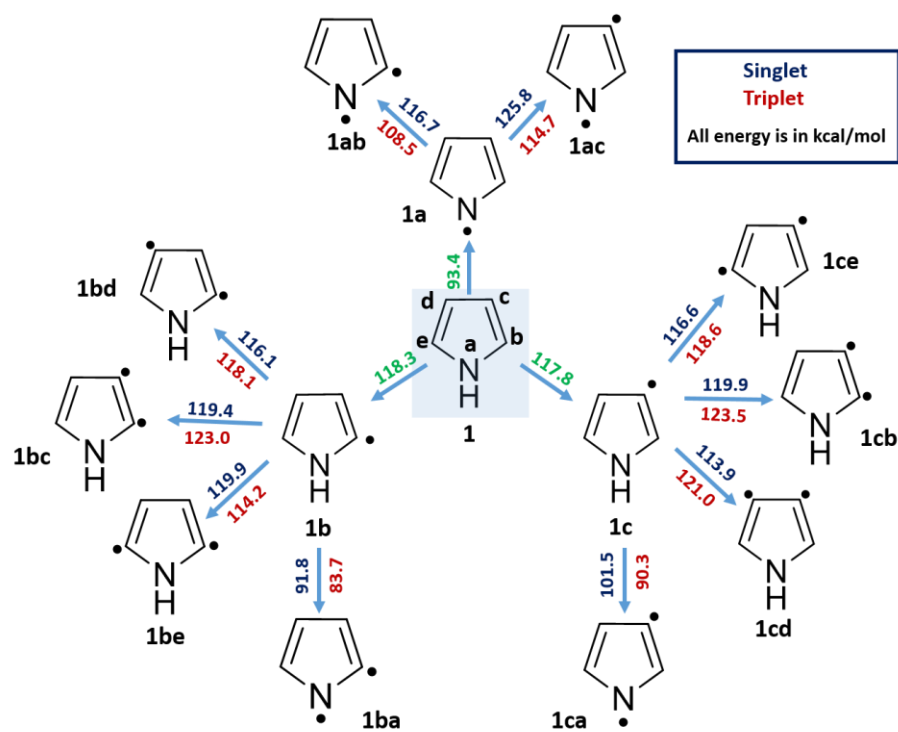


**Figure 3.9** Singlet and triplet energy gap (in kcal/mol) of didehydropyrroles at (U)B3LYP/cc-pVTZ level of theory

From **figure 3.9** we can clearly see that energy gap is more in case of biradical in which one radical is at nitrogen center (**1ab** and **1ac**). In case of nitrogen centered biradicals, triplet state gains extra stabilization through delocalization. Besides the two radical electrons are located in the orthogonal orbitals ( $\pi$  and  $\sigma$ - orbitals), and consequently, the effecting spin overlap is unfavourable. On the other hand, **1bc**, **1bd** and **1cd** singlet state is more stable because of interaction between both radical electrons (spin coupling) either through space or through bond, which leads to the stability of singlet state.

### 3.2.4 Bond Dissociation Energy

Bond dissociation energy of all the biradicals of pyrrole in singlet as well as in triplet states have been calculated at (U)B3LYP/cc-pVTZ level of theory. In case of pyrrole biradicals, there are two different paths to generate a biradical, All different ways of bond dissociation energy of biradicals have been shows in the **figure 3.10**



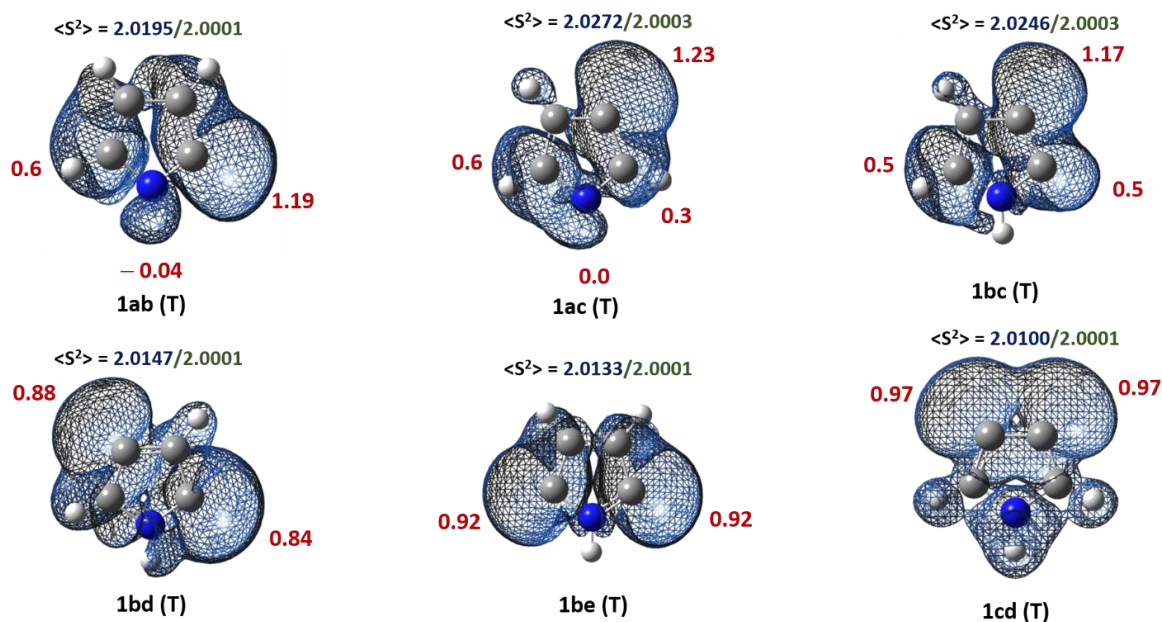
**Figure 3.10** Bond dissociation energies of pyrrole and dehydropyrrole radicals at (U)B3LYP/cc-pVTZ level of theory. Bond dissociation energy (in kcal/mol) of singlet and triplet biradical is shown in blue and red colour, respectively.

The bond dissociation energy calculations suggest that to make nitrogen centered biradicals less energy is required as compared to the other biradicals, it also confirms that the nitrogen centered biradicals are more stable. Also, lowering of BDE for triplet biradicals compared to their corresponding singlet biradicals favoured the ground states with former spin multiplicities. Except **1be**, all the carbon-centered biradicals are found to have a singlet ground state. The presence of N-H in **1be** can be comparable to the methylene or *m*-phenylene linkages in TMM and *m*-xylene biradicals, which are found to have triplet ground state as well.

### 3.2.5 Spin Density

In order to understand the nature of interaction within spins at radical centers, spin densities of all the triplet biradicals have been estimated at UB3LYP/cc-pVTZ level of theory and the results are shown in **figure 3.11**. In case of biradicals, only triplet state will show the spin density value because in singlet state difference in  $\alpha$  and  $\beta$  spin is zero. Since in triplet state difference in  $\alpha$  and  $\beta$  spin is two therefore sum of total spin of the molecule will be equal

to two. Spin contamination is also indicated in **figure 3.11** at (U)B3LYP/cc-pVTZ level of theory before and after annihilation of each biradicals in triplet state.



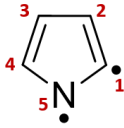
**Figure 3.11** Spin densities of didehydro-pyrrole at (U)B3LYP/cc-pVTZ level of theory. Spin contamination ( $\langle S^2 \rangle$ ) value in blue and green shows before and after annihilation respectively.

The observations depicts that the spin at nitrogen center is delocalized, whereas the spin density at carbon center is localized, except in case of **1bc**. In case of **1bc**, spin density at radical carbon, which is next to the nitrogen is delocalized to the other carbon next to nitrogen.

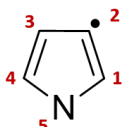
### 3.2.6 Natural Bond Orbital (NBO) Analysis

To quantify the radical-radical and radical-lone pair interactions, natural bond orbital analysis have been performed at (U)B3LYP/cc-pVTZ level of theory and all the relevant interactions have been shown in **Table 3.4**

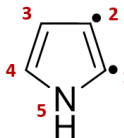
**Table 3.4** NBO of didehydro pyrrole biradicals at (U)B3LYP/cc-pVTZ level of theory

<b>1ab (Singlet)</b>				<b>1ab (Triplet)</b>		
Interactions		<E2>		Interactions		<E2>
Donor NBO	Acceptor NBO			Donor NBO	Acceptor NBO	
n (N5)	$n^*_{C1}$	17.08		n (N5)	$n^*_{C1}$	10.46
n (N5)	$\pi^*_{C1-C2}$	6.00	n (N5)	$\pi^*_{C1-C2}$	2.43	

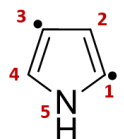
  

<b>1ac (Singlet)</b>				<b>1ac (Triplet)</b>		
Interactions		<E2>		Interactions		<E2>
Donor NBO	Acceptor NBO			Donor NBO	Acceptor NBO	
-	-	-		n (N5)	$n^*_{C2}$	0.73
-	-	-	n (N5)	$\pi^*_{C1-C2}$	4.57	

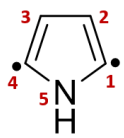
  

<b>1bc (Singlet)</b>				<b>1bc (Triplet)</b>		
Interactions		<E2>		Interactions		<E2>
Donor NBO	Acceptor NBO			Donor NBO	Acceptor NBO	
n (N5)	$\pi^*_{C1-C2}$	27.55		$n_{C1}$	$n^*_{C2}$	13.24
-	-	-	n (N5)	$n^*_{C1}$	37.79	

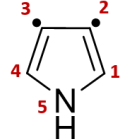
  

<b>1bd (Singlet)</b>				<b>1bd</b>		
Interactions		<E2>		Interactions		<E2>
Donor NBO	Acceptor NBO			Donor NBO	Acceptor NBO	
n (N5)	$\pi^*_{C1-C2}$	43.39		n (N5)	$\pi^*_{C1-C2}$	8.66
n (N5)	$\pi^*_{C3-C4}$	30.59	n (N5)	$\pi^*_{C3-C4}$	14.14	

<b>1be (Singlet)</b>				<b>1be</b>		
Interactions		<E2>		Interactions		<E2>
Donor NBO	Acceptor NBO			Donor NBO	Acceptor NBO	
$n_{C1}$	$n^*_{C4}$	0.88		n (N5)	$n^*_{C1}$	37.55
n (N5)	$n^*_{C1}$	36.37	n (N5)	$\pi^*_{C1-C4}$	4.54	

<b>1cd (Singlet)</b>				<b>1cd</b>		
Interactions		<E2>		Interactions		<E2>
Donor NBO	Acceptor NBO			Donor NBO	Acceptor NBO	
n (N5)	$\pi^*_{C1-C2}$	30.41		n (N5)	$\pi^*_{C1-C2}$	15.12
n (N5)	$\pi^*_{C3-C4}$	30.41	n (N5)	$\pi^*_{C3-C4}$	15.12	

In case of **1ab**, both in singlet and triplet states, significant amount of through space (TS) interaction between lone pair and radical on C<sub>1</sub> carbon shows that they are in the same plain therefore this result supports that the radical on nitrogen center is in the  $\pi$ -orbital. In **1ac**

(**singlet**), we did not find any interaction between lone pair-radical or radical-radical interactions, but in case of **1ac (triplet)** very less amount of through space interaction is there because the distance between lone pair and radical center has increased. In case of **1bc (triplet)**, radicals are at *ortho* to each other so we observed through space interaction between them. We also observed very small amount of through space interaction between radicals in **1be (singlet)**. All other through bond interaction between lone pair and radical electron is shown in **table 3.4**.



## **Chapter 4. Matrix Isolation Technique and Experimental Setup**

### **4.1 Matrix isolation**

The term “matrix isolation” was coined by George Pimentel in 1954.<sup>58</sup> The technique was firstly used for the study of free radicals but later became powerful tool for studying other reactive intermediates like carbenes, nitrenes, benzyne etc. The method involves “host-guest” analogy, in which molecules of interest (guest) are trapped in a solid inert gas matrix (host) such as argon or nitrogen and deposited on to the KBr window at temperature of ~4 K. The low temperatures can be achieved by closed cycle helium cryostat. The concentration of the sample is kept sufficiently low, typically guest and host sample ratio is kept in range 1:1000 to 1:2000 for ensuring the molecules of interest are surrounded only by the inert gas host, resulting in molecular isolation. The technique was developed to inhibit intermolecular interactions of reactive species by trapping them in a rigid cage, but it has proved to be of great importance in studying these interactions in molecular complexes. The study of weakly bound systems like hydrogen bonding, charge transfer and van der Waals complexes can also be isolated in low temperature matrices.

### **4.2 Advantage of Matrix Isolation Technique**

Inert gases are used not just because of their unreactivity with guest molecules but also of their broad optical transparency in their solid state. Inert gases used are mostly monoatomic except nitrogen, due to this they do not have any vibrational component, so they cannot interfere with IR spectra of sample. Under low temperatures, molecules do not experience intermolecular interaction because of the isolation in the solid matrix. The low temperatures also help to produce fine spectra, since only the lower electronic and vibrational quantum states are populated. The broadening due to Doppler effect and collisional broadening are reduced.

### **4.3 Instrumental Setup**

The main components of matrix isolation setup is cryostat, vacuum system and FTIR spectrometer.

### 4.3.1 Cryostat

Cryostat (RDK-408D2 from Sumitomo cryogenics) is used to get the cryogenic temperature, which is necessary to solidify the inert gas. The gases like N<sub>2</sub>, Ar, Ne, requires very low temperature to solidify. The common cryogenic fluids like liquid N<sub>2</sub>, liquid He, liquid H<sub>2</sub> are used in cryostat to obtain low temperatures. An optical part (KBr window for IR and quartz window for UV-Vis spectroscopy) is fitted to the cold head and will attain the minimum temperature due to thermal contact.

#### Helium Compressor

In our matrix isolation setup three-stage closed cycle helium compressor (Sumitomo Heavy industries Ltd.) is used to produce 4 K temperature, which is equipped with the cryostat. A water cooled helium gas compressor unit (F-70L from Sumitomo cryogenics) needs to be used in this regard to achieve the desired 4 K temperature. Compressor is connected to the cold head of the cryostat with two bellows hoses. One of the bellows hoses supplies high pressure helium gas from compressor to cryostat, other bellows tube returns low pressure helium gas from cold head to compressor.

#### Temperature Controller

A temperature controller (LakeShore model No. 336) with a temperature sensor is connected to the optical window at the cryostat cold head part, where the sample will be deposited. This has the possibility to heat the window to desired temperature to perform annealing experiments, where the solid inert gases are allowed to soften such that the diffusion of the trapped species can be enabled.

### 4.3.2 Vacuum System

There are two types of pumping system employed in this setup.

- a) Oil rotary vane pump
- b) Diffusion pump

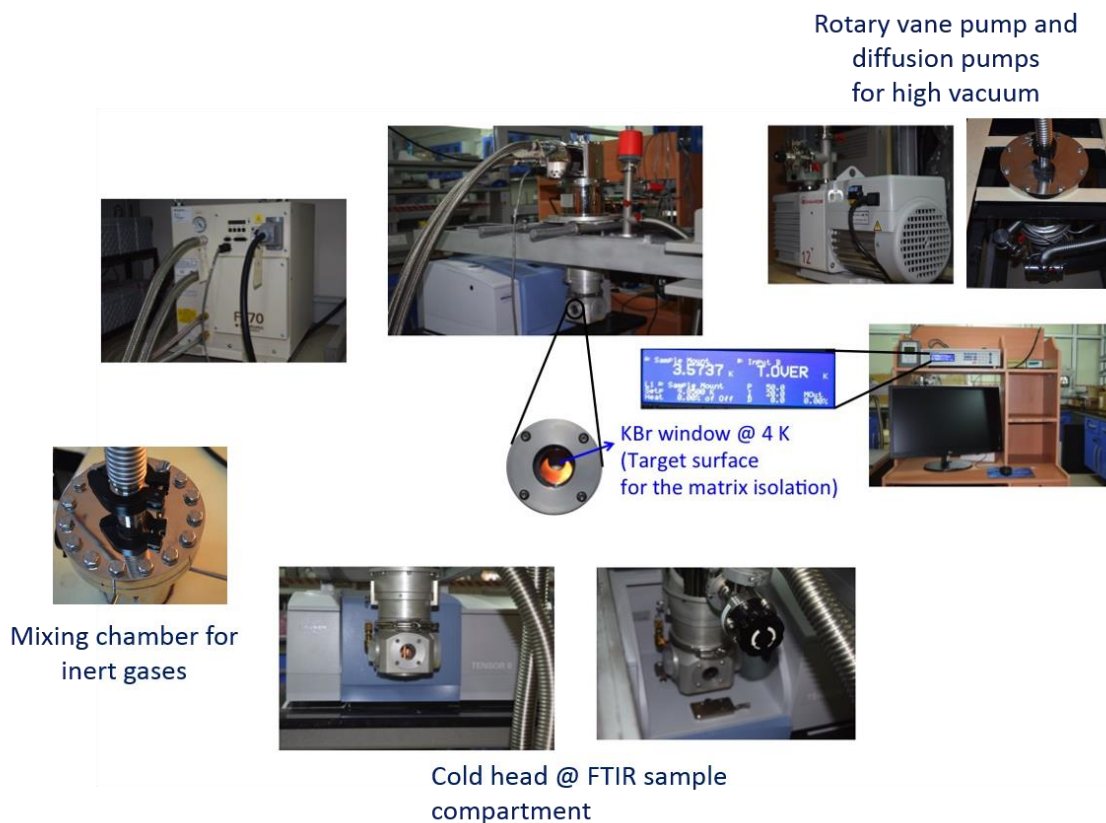
Rotary pumps are basically mechanical pumps, which can remove the air molecules from the system by rotary-vane devices. The average vacuum can maintained by this pump is around 10<sup>-3</sup> bar. These pumps have mainly two purpose: a) they remove bulk of the air which is

initially at atmospheric pressure b) since diffusion pump cannot exhaust against atmospheric pressure so backing of diffusion pump is used. The pumping speed of rotary pumps are 100 lit/min.

Diffusion pump can reach and maintain a vacuum around  $10^{-6}$  bar. The pumping speed of diffusion pump is 280lit/min and it backed by rotary pump. it is made up of stainless steel chamber containing vertically stacked cone-shaped jet assemblies. At the base of chamber there is a oil container in which generally silicon oil used. Oil has very low vapour pressure and it is heated by an electric heater. The vapour of the oil move upward and is expelled through jet assemblies. To cool the chamber, cold water flow around the chamber through the coil outside coil.

### 4.3.3 FTIR Spectrometer

A Bruker Tensor II FTIR spectrometer has been installed for recording the IR spectra.



**Figure 4.1** Parts of matrix isolation setup

# Chapter 5. Summary and Outlook

## 5.1 Summary

The electronic structure and stability patterns of dehydro- pyrrole, furan, thiophene and borole radical isomers have been investigated using quantum chemical calculations. The analysis of geometrical parameters gives insights about the changes in the structural aspects as an effect of radical formation, which also gives some hints about the interaction of radical with atomic centers. The stability order of all the radical isomers were determined and compared among each molecule. Moreover, the overall stability has been compared using isodesmic reactions. The spin density and electrostatic potential diagram depicted the distribution of electron density over the molecule, which in turn gives a qualitative picture of the interaction of radical center. The CASSCF calculations illustrate the molecular orbital picture and the characteristic type of interaction at the radical center with rest of the molecule, especially when looking at the SOMO. A clear quantitative picture has been obtained using the natural bond analysis.

Apart from the structural aspects of these radical isomers, the reactivity traits also been investigated for dehydropyrrole radical isomers. The unimolecular decomposition studies of both **1b** and **1c** gives us an idea about the kinetic stability of the radical isomers.

Furthermore, the electronic structural studies of didehydropyrrole biradicals have also been carried out for understanding the radical-radical interactions, apart from the radical-heteroatom interaction. The geometrical paramaters, stability pattern, spin density and NBO analysis have been investigated for all the possible biradical isomers of pyrrole. Besides these calculations the singlet-triplet energy gap also been determined for better understanding of the ground state spin multiplicites.

Exploration of the structure and stability patterns of the radical isomers of pyrrole, furan, thiophene and borole suggests that the radical isomer, which is having the radical center over the heteroatom, is more stable than at carbon centered. The carbon centered radicals show energy values that are close to each other, as compared to the N/B centered radical. The isodesmic reaction studies shows that the N-centered radical is the most stable among all

radicals. The stability of these N/B centered radicals can be attributed to the delocalization of electron density, which is obtained through the spin density calculations. The molecular orbitals obtained from the CASSCF calculations also confirmed this. Both N/B centered radical forms a  $\pi$  radical, whereas all the other C-centered radicals form a  $\sigma$  radical.

Besides the thermodynamic stability analysis, the kinetic stability of pyrrole radical has also been examined by determining the unimolecular decomposition pathways. The difficulty in determining the decomposition pathways of N-centered radical (**1a**) reassures the stability of the radical isomer. In both **1b** and **1c** the pathway containing the cleavage of C-N bond found to be kinetically more favorable than C-C bond breakage.

The extent of radical-radical interaction has been investigated by analysing the didehydro-pyrrole biradical systems. The energy calculations using isodesmic reactions suggest that the biradical involving the N-centered radical is more stable irrespective of the spin state of the system. Interestingly, the triplet state of N-centered biradicals are significantly stabilized over the singlet state, whereas the all C-centered biradicals prefer a singlet ground state. This stabilization pattern can be explained using the delocalization of the radical electron from the formal radical center at nitrogen to the ring, which is clearly depicted in spin density figure. Moreover the lower bond dissociation energy for the formation of biradical confirms this extra stability of N-centered biradicals.

## 5.2 Outlook

Based on our computational studies the most significant result that we obtained was the accumulation and delocalization of radical electron in  $\pi$ -orbitals of N-centered radical of pyrrole **1a**. Many levels of theory confirmed the same results. The extension of this in creating biradicals with one of center at nitrogen proves that the resulting molecules attain high spin triplet state. This interesting results need to be confirmed at other levels of theory. Once proven, such biradical moieties can be incorporated in designing new type of organic molecular magnets. Apart from that these biradicals need to be confirmed through experiments like matrix isolation infrared spectroscopy.

---

## References

1. Gomberg, M. Organic Radicals. *Chem. Rev.* **1924**, *1*, 91-141
2. Wentrup, C. From Reactive Intermediates to Stable Compounds. *Science.* **2002**, *295*, 1846-1847
3. Moss, R. A.; Platz, M. S.; Jones Jr, M. *Reactive Intermediates in Chemistry.*; John Wiley & Sons, Ltd: New York, **2003**
4. Crossley, S. W. M.; Obradors, C.; Martinez, R. M.; Shenvi, R. A. Mn-, Fe-, and Co-Catalyzed Radical Hydrofunctionalizations of Olefins. *Chem. Rev.* **2016**, *116*, 8912-9000
5. Yan, M.; Lo, J. C.; Edwards, J. T.; Baran, P. S. Radicals: Reactive Intermediates with Translational Potential. *J. Am. Chem. Soc.* **2016**, *138*, 12692-12714
6. Omero, N. A.; Nicewicz, D. A. Organic Photoredox Catalysis. *Chem. Rev.* **2016**, *116*, 10075-10166
7. Matyjaszewski, K.; Xia, J. Atom Transfer Radical Polymerization. *Chem. Rev.* **2001**, *101*, 92921-2990
8. Khelifa, F.; Ershov, S.; Habibi, Y.; Snyders, R.; Dubois, P. Free Radical Induced Grafting from Plasma Polymer Surfaces. *Chem. Rev.* **2016**, *116*, 3975-4005
9. Orlando, J. J.; Tyndall, G. S. The Atmospheric Chemistry of Alkoxy Radicals. *Chem. Rev.* **2003**, *103*, 4657-4689
10. Gligorovski, S.; Strekowski, R.; Barbati, S.; Vione, D. Environmental Implications of Hydroxyl Radicals ( $\bullet\text{OH}$ ). *Chem. Rev.* **2015**, *115*, 13051-13092
11. Imlay, J. A.; Linn, S. DNA Damage and Oxygen Radical Toxicity. *Science.* **1988**, *240*, 1302-1309
12. Davies, K. J.; Pryor, W. A. The Evolution of Free Radical Biology and Medicine: A 20-Year History. *Free Radic. Biol. Med.* **2005**, *39*, 1263-1264
13. Gomberg, M. An Instance of Trivalent Carbon: Triphenylmethyl. *J. Am. Chem. Soc.* **1900**, *22*, 757-771
14. Vleeschouwer, F. D.; Chankisjijev, A.; Yang, W.; Geerlings, P.; Proft, F. D. Pushing the Boundaries of Intrinsically Stable Radicals: Inverse Design Using the Thiadiazinyl Radical as a Template. *J. Org. Chem.* **2013**, *78*, 3151-3158

15. Fadden, M. J.; Hadad, C. M. Rearrangement Pathways of Arylperoxy Radicals. 2. Five-Membered Heterocycles. *J. Phys. Chem. A* **2000**, *104*, 6324-6331
16. Vasiliou, A.; Nimlos, M. R.; Daily, J. W.; Ellison, G. B. Thermal Decomposition of Furan Generates Propargyl Radicals. *J. Phys. Chem. A* **2009**, *113*, 8540-8547
17. Mukhopadhyay, A.; Jacob, L.; Venkataramani, S. Dehydro-Oxazole, Thiazole and Imidazole radicals; An Insight into the Electronic Structure, Stability and Reactivity Aspects. *Phys. Chem. Chem. Phys.* **2017**, *19*, 394-407
18. McFadden, B. D.; Arce, M. M.; Carnicom, E. M.; Herman, J.; Abrusezze, J.; Tillman, E. S. Radical Trap-Assisted Atom Transfer Radical Coupling of Diblock Copolymers as a Method of Forming Triblock Copolymers. *Macromol. Chem. Phys.* **2016**, *217*, 2473-2482
19. Mackie, I. D.; Dilabio, G. A. Ring- opening radical clock reactions: many density functionals have difficulty keeping time. *Org. Biomol. Chem.* **2011**, *9*, 3158-3164
20. Buettner G. R. The Spin Trapping of Superoxide and Hydroxyl Free Radical with DMPO (5, 5-Dimethylpyrroline-N-oxide): More about Iron. *Free. Radic. Res. Commun.* **1993**, *19*, 79-87
21. Dougherty, D. A. Spin Control in Organic Molecules. *Acc. Chem. Res.* **1991**, *24*, 88-94
22. Rajca, A. Organic Diradicals and Polyradicals: From Spin Coupling to Magnetism? *Chem. Rev.* **1994**, *94*, 871-893
23. Cristian, A. C.; Shao, Y.; Krylov, A. I. Bonding Patterns in Benzene Triradicals from Structural, Spectroscopic, and Thermochemical Perspectives. *J. Phys. Chem. A* **2004**, *108*, 6581-6588
24. Ma, H.; Liu, C.; Zhang, C.; Jiang, Y. Theoretical Study of Very High Spin Organic Conjugated Polyradicals. *J. Phys. Chem. A* **2007**, *111*, 9471-9478
25. Slipchenko, L. V.; Munsch, T. E.; Wenthold, P. G.; Krylov, A. L. 5-Dehydro-1,3-Quinodimethane: A Hydrocarbon with an Open-shell Doublet Ground State. *Angew. Chem. Int. Ed. Engl.* **2004**, *43*, 742-745
26. Iwamura, H.; Koga, N. Studies of Organic Di-, Oligo-, and Polyradicals by Means of Their Bulk Magnetic Properties. *Acc. Chem. Res.* **1993**, *26*, 346-351

27. Liu, R.; Huang, T. T. S.; Tittle, J.; Xia, D. A Theoretical Investigation of the Decomposition Mechanism of Pyridyl Radicals *J. Phys. Chem. A* **2000**, *104*, 8368-8374
28. Hoffmann, R.; Imamura, A.; Hehre, W. J. Benzynes, dehydroconjugated molecule, and the interaction of orbitals separated by a number of intervening sigma bonds. *J. Am. Chem. Soc.* **1968**, *90*, 1499-1509
29. Krylov, A. I. Triradicals. *J. Phys. Chem. A* **2005**, *109*, 10638-10645
30. Hirai, K.; Itoh, T.; Tomioka, H. Persistent Triplet Carbenes. *Chem. Rev.* **2009**, *109*, 3275-3332
31. Dubnikova, F.; Lifshitz, A. Isomerization of Pyrrole. Quantum Chemical Calculations and Kinetic Modeling. *J. Phys. Chem. A* **1998**, *102*, 10880-10888
32. Dubnikova, F.; Lifshitz, A. Ring Expansion in Methylene Pyrrole Radicals. Quantum Chemical Calculations. *J. Phys. Chem. A* **2000**, *104*, 530-538
33. Zhai, L.; Zhou, X.; Liu, R. A Theoretical Study of Pyrolysis Mechanisms of Pyrrole *J. Phys. Chem. A* **1999**, *103*, 3917-3922
34. Kim, Y. S.; Inui, H.; McMahon, R. J. Ring Opening of 2, 5-Didehydrothiophene: Matrix Photochemistry of C<sub>4</sub>H<sub>2</sub>S Isomers. *J. Org. Chem.* **2006**, *71*, 9602-9608
35. Sendt, K.; Bacskay, G. B.; Mackie, J. C. Pyrolysis of Furan: Ab Initio Quantum Chemical and Kinetic Modeling Studies. *J. Phys. Chem. A*, **2000**, *104*, 1861-1875
36. Braunschweig, H.; Kupfer, T. Recent developments in the chemistry of antiaromatic boroles. *Chem. Commun.* **2011**, *47*, 10903-10914
37. Lu, D.; Wu, C.; Li, P. 3-Center-5-Electron Boryl Radicals with  $\sigma^0\pi^1$  Ground State Electronic Structure. *Org. Lett.* **2014**, *16*, 1486-1489
38. Feng, Y.; Wang, J. -T.; Liu, L.; Guo, Q. -X. C-H and N-H bond dissociation energies of five- and six-membered ring aromatic compounds. *J. Phys. Org. Chem.* **2003**, *16*, 883-890
39. Kozilol, L.; Mozhayskiy, V. A.; Braam, B. J.; Bowman, J. M.; Krylov, A. I. Ab initio calculation of photoelectron spectra of the hydroxycarbenediradicals. *J. Phys. Chem. A* **2009**, *113*, 7802-7809
40. Costa, P.; Sander, W. Hydrogen bonding switches the spin state of diphenylcarbene from triplet to singlet *Angew. Chem. Int. Ed.* **2014**, *53*, 5122-5125



- 
41. Sander, W.; Winkler, M.; Cakir, B.; Grote, D.; Bettinger, H. F. Dehydrophenylnitrenes: Matrix isolation and photochemical rearrangements. *J. Org. Chem.* **2006**, *72*, 715-724
  42. Bettinger, H. F.; Sander, W. Dehydrophenylnitrenes: Electronic and molecular structure. *J. Am. Chem. Soc.* **2003**, *125*, 9726-9733
  43. Rau, N. J.; Wenthold, P. G. Experimental investigation of the absolute enthalpies of formation of 2,3-, 2,4-, and 3,4-pyridynes. *J. Phys. Chem. A.* **2011**, *115*, 10353-10362
  44. Wenthold, P. G. Spin-state dependent radical stabilization in nitrenes; the unusually small singlet-triplet splitting in 2-furanylnitrene. *J. Org. Chem.* **2012**, *77*, 208-214
  45. Soleilhavoup, M.; Bertrand, G. Cyclic (Alkyl)(Amino)Carbene (CAACs): Stable Carbene on the Rise. *Acc. Chem. Res.* **2015**, *48*, 256-266
  46. Kirmse, W. Persistent Triplet Carbene. *Angew. Chem. Int. Ed.* **2003**, *42*, 2117-2119
  47. Szabo, A.; Ostlund, N.S. *Modern Quantum Chemistry*; Macmillan publishing company: Newyork. **1982**.
  48. Hohenberg, P.; Kohn, W. Inhomogeneous Electron Gas. *Phys. Rev.* **1964**, *136*, B864
  49. West, D.; Sun, Y. Y.; Zhang, S. B. Importance of the correct Fermi energy on the calculation of defect formation energies in Semiconductors. *Appl. Phys. Lett.* **2012**, *101*, 082105-082109
  50. Parr, R. G.; Weitao, Y. *Density-Functional Theory of Atoms and Molecules*; Oxford University Press: USA. **1994**.
  51. Kendall, R. A.; Dunning Jr, T. H.; Harrison, R. J. Electron Affinities of the First-Row Atoms Revisited. Systematic Basis Sets and Wave Functions. *J. Chem. Phys.* **1992**, *96*, 6796-6806
  52. Weinhold, F. Natural bond orbital analysis: A critical overview of relationships to alternative bonding perspectives. *J. Comput. Chem.* **2012**, *33*, 2363-2379
  53. Frisch, M. J.; Trucks, G. W.; Schlegel, H. B.; Scuseria, G. E.; Robb, M. A.; Cheeseman, J. R.; Scalmani, G.; Barone, V.; Petersson, G. A.; Nakatsuji, H. *et al.* *Gaussian 09*, Revision C. 01; Gaussian, Inc.; Wallingford, CT, **2009**.
  54. Foster, J. P.; Weinhold, F. Natural hybrid orbitals. *J. Am. Chem. Soc.* **1980**, *102*, 7211-7218

- 
55. Werner, H. J.; Knowles, P. J.; Knizia, G.; Manby, F. R.; Schütz, M.; Celani, P.; Györffy, W.; Kats, D.; Korona, T.; Lindh, R. *MOLPRO*, Version 2012.1, A Package Of *Ab Initio* Programs, **2012**
56. Werner, H. J.; Knowles, P. J.; Knizia, G.; Manby, F. R.; Schutz, M. Molpro: A General-Purpose Quantum Chemistry Program Package, *WIREs Comput Mol Sci* **2**, **2012**, 242-253
57. Hehre, W. J.; R. Ditchfield, R.; L. Radom, L.; Pople, J. A. Molecular orbital theory of the electronic structure of organic compounds. V. Molecular theory of bond separation. *J. Am. Chem. Soc.* **1970**, *92*, 4796-4801
58. Whittle, E.; Dows, D. A.; Pimentel, G. C. Matrix Isolation Method for the Experimental Study of Unstable Species. *J. Chem. Phys.* **1954**, *22*, 1943

# Appendix

Cartesian coordinates of the optimized structures at UB3LYP/cc-pVTZ level of theory.

## Pyrrole (1)

Atoms	X	Y	Z
C	0.000000	1.121630	0.330549
C	0.000000	0.710486	-0.979843
C	0.000000	-0.710486	-0.979843
C	0.000000	-1.121630	0.330549
N	0.000000	0.000000	1.118484
H	0.000000	0.000000	2.121709
H	0.000000	2.107048	0.761623
H	0.000000	1.355883	-1.841405
H	0.000000	-1.355883	-1.841405
H	0.000000	-2.107048	0.761623

## 1-dehydro-pyrrole (1a)

Atoms	X	Y	Z
C	0.000000	1.061684	0.423823
C	0.000000	0.678486	-0.981086
C	0.000000	-0.678486	-0.981086
C	0.000000	-1.061684	0.423823
N	0.000000	0.000000	1.243511
H	0.000000	2.069203	0.816049
H	0.000000	1.348653	-1.824762
H	0.000000	-1.348653	-1.824762
H	0.000000	-2.069203	0.816049

## 2-dehydro-pyrrole (1b)

Atoms	X	Y	Z
C	0.000000	1.120862	0.000000
C	1.107406	0.311719	0.000000
C	0.672950	-1.053886	0.000000
C	-0.687448	-0.982498	0.000000
N	-1.115278	0.302214	0.000000
H	-2.071322	0.605996	0.000000
H	-0.096902	2.192099	0.000000
H	2.131618	0.645689	0.000000
H	1.286107	-1.936463	0.000000

**3-dehyydro-pyrrole (1c)**

Atoms	X	Y	Z
C	-1.085786	0.230319	0.000000
C	-0.637367	-1.075464	0.000000
C	0.765233	-0.976629	0.000000
C	1.166173	0.326250	0.000000
N	0.000000	1.065044	0.000000
H	-0.047135	2.068248	0.000000
H	-2.088962	0.620394	0.000000
H	-1.248908	-1.960033	0.000000
H	2.135487	0.789224	0.000000

**Furan (2)**

Atoms	X	Y	Z
C	0.000000	1.092702	0.345703
C	0.000000	0.715990	-0.955573
C	0.000000	-0.715990	-0.955573
C	0.000000	-1.092702	0.345703
H	0.000000	2.046827	0.840331
H	0.000000	1.370090	-1.809989
H	0.000000	-1.370090	-1.809989
H	0.000000	-2.046827	0.840331
O	0.000000	0.000000	1.157219

**2-dehydro-furan (2b)**

Atoms	X	Y	Z
C	0.000000	1.122794	0.000000
C	1.113326	0.315700	0.000000
C	0.650908	-1.065935	0.000000
C	-0.723751	-0.974046	0.000000
H	-0.146377	2.209213	0.000000
H	2.156378	0.646123	0.000000
H	1.262338	-1.970480	0.000000
O	-1.189404	0.340508	0.000000

**3-dehydro-furan (2c)**

Atoms	X	Y	Z
C	0.000000	1.112633	0.000000
C	1.182984	0.407380	0.000000
C	0.786100	-0.985280	0.000000
C	-0.581215	-1.062135	0.000000
H	-0.226644	2.185773	0.000000
H	2.195294	0.818615	0.000000
H	-1.307656	-1.880969	0.000000
O	-1.123526	0.255124	0.000000

**Thiophene (3)**

Atoms	X	Y	Z
C	0.000000	1.238003	-0.009748
C	0.000000	0.711484	-1.267050
C	0.000000	-0.711484	-1.267050
C	0.000000	-1.238003	-0.009748
S	0.000000	0.000000	1.192779
H	0.000000	2.274519	0.281224
H	0.000000	1.314856	-2.162674
H	0.000000	-1.314856	-2.162674
H	0.000000	-2.274519	0.281224

**2-dehydro-thiophene (3b)**

Atoms	X	Y	Z
C	0.000000	1.192001	0.000000
C	1.273612	0.683923	0.000000
C	1.306006	-0.778371	0.000000
C	0.034153	-1.279565	0.000000
H	-0.296614	2.244612	0.000000
H	2.179767	1.301020	0.000000
H	2.226846	-1.370594	0.000000
S	-1.237039	-0.067685	0.000000

**3-dehydro-thiophene (3c)**

Atoms	X	Y	Z
C	-1.212705	-0.104708	0.000000
C	-0.669769	-1.367844	0.000000
C	0.778691	-1.292958	0.000000
C	1.300568	-0.036933	0.000000
H	-2.275270	0.156430	0.000000
H	-1.250633	-2.296177	0.000000
H	2.345190	0.283654	0.000000
S	0.000000	1.166922	0.000000

**Borole (4)**

Atoms	X	Y	Z
C	0.000000	1.251046	0.348024
C	0.000000	0.757701	-0.896244
C	0.000000	-0.757701	-0.896244
C	0.000000	-1.251046	0.348024
H	0.000000	0.000000	2.502398
H	0.000000	2.307381	0.572946
H	0.000000	1.327466	-1.818166
H	0.000000	-1.327466	-1.818166
H	0.000000	-2.307381	0.572946
B	0.000000	0.000000	1.313336

**1-dehydro-borole (4a)**

Atoms	X	Y	Z
C	-0.050611	-0.467552	1.297097
C	-0.050611	0.784713	0.743963
C	-0.050611	0.784713	-0.743963
C	-0.050611	-0.467552	-1.297097
H	-0.008447	-0.701127	2.344782
H	0.048447	1.708732	1.301622
H	0.048447	1.708732	-1.301622
H	-0.008447	-0.701127	-2.344782
B	0.226931	-1.164228	0.000000

**2-dehydro-borole (4b)**

Atoms	X	Y	Z
C	1.154684	0.424558	0.000000
C	0.000000	1.108992	0.000000
C	-1.223125	0.188689	0.000000
C	-0.796238	-1.063349	0.000000
H	1.498704	-2.053961	0.000000
H	2.125153	0.899439	0.000000
H	-0.109718	2.187974	0.000000
H	-2.237329	0.566804	0.000000
B	0.782253	-1.110719	0.000000

**3-dehydro-borole (4c)**

Atoms	X	Y	Z
C	-0.746020	1.001510	0.000000
C	-1.187082	-0.261251	0.000000
C	0.000000	-1.186217	0.000000
C	1.201382	-0.631091	0.000000
H	1.619676	1.808878	0.000000
H	-1.393771	1.867076	0.000000
H	-2.207307	-0.618152	0.000000
H	2.155266	-1.134151	0.000000
B	0.843291	0.907729	0.000000

**1,2-didehydro-pyrrole (1ab) Singlet**

Atoms	X	Y	Z
C	0.031826	-1.042081	0.187265
C	1.205387	-0.354935	-0.106734
C	0.604657	0.914494	-0.001891
C	-0.814156	0.734272	-0.016350
N	-1.135129	-0.596615	-0.097025
H	2.235563	-0.645971	-0.045622
H	1.125902	1.838178	0.202944
H	-1.581844	1.473604	0.148108

**1,2-didehydro-pyrrole (1ab) Triplet**

Atoms	X	Y	Z
C	-0.423290	-1.194646	0.000000
C	0.915605	-0.779597	0.000000
C	0.915605	0.653983	0.000000
C	-0.423290	1.069032	0.000000
N	-1.234292	-0.062807	0.000000
H	1.789486	-1.422376	0.000000
H	1.789486	1.296762	0.000000
H	-0.846703	2.072637	0.000000

**1,3-didehydro-pyrrole (1ac) Singlet**

Atoms	X	Y	Z
C	-1.222860	-0.489650	0.000000
C	0.000000	-1.011447	0.000000
C	1.222634	-0.366814	0.000000
C	0.655946	0.893915	0.000000
N	-0.715626	0.786986	0.000000
H	2.221097	-0.756547	0.000000
H	1.105407	1.872907	0.000000
H	-2.251443	-0.781289	0.000000

**1,3-didehydro-pyrrole (1ac) Triplet**

Atoms	X	Y	Z
C	0.724156	0.951160	0.000000
C	-0.743763	0.961740	0.000000
C	-1.197753	-0.324856	0.000000
C	0.000000	-1.078874	0.000000
N	1.146851	-0.287101	0.000000
H	-2.208352	-0.692984	0.000000
H	0.097879	-2.154954	0.000000
H	1.386676	1.802628	0.000000

**2,3-didehydro-pyrrole (1bc) Singlet**

Atoms	X	Y	Z
C	-0.750058	-0.973440	0.090250
C	0.491382	-1.113979	-0.089772
C	1.206495	0.102218	0.056609
C	0.177717	1.036085	0.005406
N	-1.043866	0.355734	-0.067494
H	-1.934150	0.783297	0.126212
H	2.261014	0.306578	0.006254
H	0.226981	2.114681	-0.034963

**2,3-didehydro-pyrrole (1bc) Triplet**

Atoms	X	Y	Z
C	-0.674293	-1.127502	0.000000
C	0.740545	-0.998810	0.000000
C	1.183009	0.307938	0.000000
C	0.000000	1.060694	0.000000
N	-1.071768	0.176007	0.000000
H	-2.034433	0.472218	0.000000
H	2.182439	0.708831	0.000000
H	-0.141196	2.132986	0.000000

**2,4-didehydro-pyrrole (1bd) Singlet**

Atoms	X	Y	Z
C	0.000000	1.056615	0.000000
C	-1.259508	0.523419	0.000000
C	-0.759575	-0.760162	0.000000
C	0.586669	-1.027160	0.000000
N	1.093075	0.236156	0.000000
H	2.041684	0.567010	0.000000
H	-2.228875	0.976697	0.000000
H	1.130146	-1.953075	0.000000

**2,4-didehydro-pyrrole (1bd) Triplet**

Atoms	X	Y	Z
C	0.374312	-1.100408	0.084201
C	1.270895	-0.023429	-0.001268
C	0.462750	1.107178	-0.011891
C	-0.868762	0.749004	0.001379
N	-0.898940	-0.631963	-0.080660
H	-1.727544	-1.193747	0.018486
H	2.338660	-0.100977	-0.102417
H	-1.753703	1.324393	0.214024



**2,5-didehydro-pyrrole (1be) Singlet**

Atoms	X	Y	Z
C	-0.088990	0.407802	1.058888
C	-0.088990	-0.973304	0.685228
C	-0.088990	-0.973304	-0.685228
C	-0.088990	0.407802	-1.058888
N	0.343874	1.167618	0.000000
H	0.197063	2.165410	0.000000
H	-0.234215	-1.776360	1.388667
H	-0.234215	-1.776360	-1.388667

**2,5-didehydro-pyrrole (1be) Triplet**

Atoms	X	Y	Z
C	0.000000	1.117136	0.400420
C	0.045557	0.680929	-0.972188
C	-0.045557	-0.680929	-0.972188
C	0.000000	-1.117136	0.400420
N	0.000000	0.000000	1.183425
H	0.000000	0.000000	2.187332
H	0.116753	1.360313	-1.805047
H	-0.116753	-1.360313	-1.805047

**3,4-didehydro-pyrrole (1cd) Singlet**

Atoms	X	Y	Z
C	0.000000	1.138189	0.208560
C	0.000000	0.631998	-1.069671
C	0.000000	-0.631998	-1.069671
C	0.000000	-1.138189	0.208560
N	0.000000	0.000000	1.008704
H	0.000000	0.000000	2.018593
H	0.000000	2.127468	0.626903
H	0.000000	-2.127468	0.626903

**3,4-didehydro-pyrrole (1cd) Triplet**

Atoms	X	Y	Z
C	0.000000	1.132651	0.219651
C	0.000000	0.709331	-1.080581
C	0.000000	-0.709331	-1.080581
C	0.000000	-1.132651	0.219651
N	0.000000	0.000000	1.004563
H	0.000000	0.000000	2.009127
H	0.000000	2.120077	0.645046
H	0.000000	-2.120077	0.645046